



Published in final edited form as:

Cell Rep. 2018 January 09; 22(2): 456–470. doi:10.1016/j.celrep.2017.12.044.

PlexinA2 Forward Signaling through Rap1 GTPases Regulates Dentate Gyrus Development and Schizophrenia-like Behaviors

Xiao-Feng Zhao¹, Rafi Kohen^{1,9}, Rachel Parent², Yuntao Duan¹, Grace L. Fisher², Matthew J. Korn³, Lingchao Ji⁴, Guoqiang Wan⁴, Jing Jin^{5,6}, Andreas W. Püschel^{5,6}, David F. Dolan⁴, Jack M. Parent^{3,7,9}, Gabriel Corfas^{4,9}, Geoffrey G. Murphy^{2,8,9}, and Roman J. Giger^{1,3,9,10,*}

¹Department of Cell and Developmental Biology

²Molecular & Behavioral Neuroscience Institute

³Department of Neurology

⁴Kresge Hearing Research Institute University of Michigan, Ann Arbor, MI 48109, USA

⁵Institut für Molekulare Zellbiologie, Westfälische Wilhelms-Universität, 48149 Münster, Germany

⁶Cells-in-Motion Cluster of Excellence, University of Münster, 48149 Münster, Germany

⁷VA Ann Arbor Healthcare System, Ann Arbor, MI 48105, USA

⁸Department of Molecular and Integrative Physiology, University of Michigan, Ann Arbor, MI 48109, USA

⁹Neuroscience Graduate Program University of Michigan, Ann Arbor, MI 48109, USA

SUMMARY

Dentate gyrus (DG) development requires specification of granule cell (GC) progenitors in the hippocampal neuroepithelium, as well as their proliferation and migration into the primordial DG. We identify the Plexin family members *Plxna2* and *Plxna4* as important regulators of DG development. Distribution of immature GCs is regulated by Sema5A signaling through PlxnA2 and requires a functional PlxnA2 GTPase-activating protein (GAP) domain and Rap1 small GTPases. In adult *Plxna2*^{-/-} but not *Plxna2-GAP*-deficient mice, the dentate GC layer is severely malformed, neurogenesis is compromised, and mossy fibers form aberrant synaptic boutons within

This is an open access article under the CC BY-NC-ND license (<http://creativecommons.org/licenses/by-nc-nd/4.0/>).

*Correspondence: rgiger@umich.edu.

¹⁰Lead Contact

SUPPLEMENTAL INFORMATION

Supplemental Information includes a detailed description of Supplemental Experimental Procedures and eight figures and can be found with this article online at <https://doi.org/10.1016/j.celrep.2017.12.044>.

AUTHOR CONTRIBUTIONS

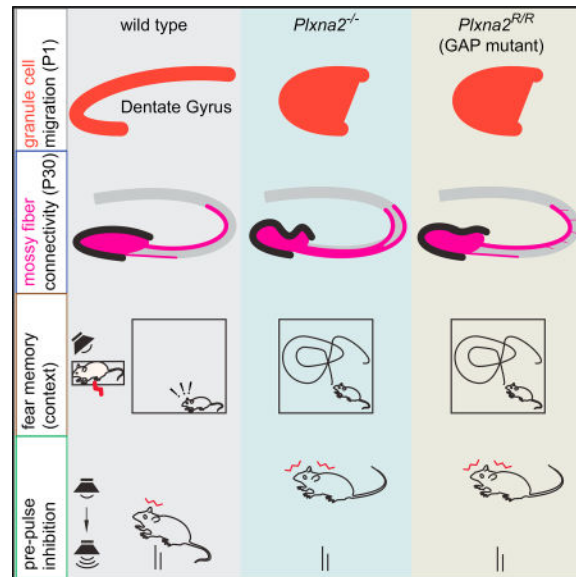
X.-F.Z. and R.J.G. designed experiments. X.-F.Z., R.K., R.P., Y.D., G.L.F., M.J.K., L.J., and G.W. conducted experiments. J.J. and A.W.P. provided *Rap1* mouse reagents. X.-F.Z., R.K., R.P., D.F.D., J.M.P., G.C., G.G.M., and R.J.G. analyzed data. R.J.G. wrote the manuscript.

DECLARATION OF INTERESTS

G.C. is a scientific founder of Decibel Therapeutics; he has an equity interest in and has received compensation for consulting. The company was not involved in this study.

CA3. Behavioral studies with *Plxna2*^{-/-} mice revealed deficits in associative learning, sociability, and sensorimotor gating—traits commonly observed in neuropsychiatric disorder. Remarkably, while morphological defects are minimal in *Plxna2-GAP*-deficient brains, defects in fear memory and sensorimotor gating persist. Since allelic variants of human *PLXNA2* and *RAP1* associate with schizophrenia, our studies identify a biochemical pathway important for brain development and mental health.

In Brief



Zhao et al. find that Sema5A-PlexinA2 forward signaling through Rap1 GTPases is required for progenitor distribution in the developing mouse dentate gyrus. Adult *Plxna2*^{-/-}, but not *Plxna2-GAP*-deficient, mice show defects in dentate morphology, neurogenesis, and mossy fiber connectivity. *Plxna2*^{-/-} and *Plxna2-GAP* mice exhibit behavioral defects suggestive of neuropsychiatric illness.

INTRODUCTION

There is overwhelming evidence that neuropsychiatric disorders have a developmental origin with a strong genetic underpinning (Wray and Gottesman, 2012). The genetic architecture of schizophrenia (SCZ), bipolar disorder, and autism spectrum disorder is polygenic and highly heterogeneous, involving a mixture of rare and common risk alleles (Henriksen et al., 2017). Recent success in gene discovery poses new challenges, including the characterization of biochemical pathways altered by disease alleles and developing a deeper understanding of the associated biology in the context of disease.

Developmental processes associated with neuropsychiatric illness include cell migration, axon guidance, cell adhesion, synaptogenesis, and neurotransmission (Chang et al., 2015; English et al., 2011; Yin et al., 2012). Allelic variants for members of the *SEMAPHORIN* (*SEMA*) family of axon guidance molecules and their receptors, the *PLEXINS* (*PLXNs*),

have been associated with mental disorder. These include SNPs in *SEMA5A* and its receptor *PLXNA2* (Mah et al., 2006; Weiss et al., 2009). Mice deficient for *Plxna2* show defects in dentate gyrus (DG)-CA3 connectivity in the adult hippocampus (Duan et al., 2014; Suto et al., 2007; Tawarayama et al., 2010), cerebellar granule cell migration (Renaud et al., 2008), and accessory optic system development (Sun et al., 2015). Whether morphological defects in *Plxna2*^{-/-} mice impact brain function or cause behavioral defects suggestive of neuropsychiatric illness, however, has not yet been examined.

The Plxns are a large family of type-1 transmembrane proteins, members of which function as canonical Sema receptors (Pasterkamp, 2012; Riccomagno and Kolodkin, 2015). In addition to their receptor function, Plxns can operate as ligands for transmembrane Semas, participating in “reverse signaling” (Battistini and Tamagnone, 2016). Structural studies revealed that, in the absence of Sema ligand, the Plxn extracellular portion rests in an auto-inhibitory conformation (Kong et al., 2016). Ligand binding leads to Plxn dimerization (Wang et al., 2012) and activation of an intrinsic GTPase-activating protein (GAP) domain located within the cytoplasmic region. The Plxn GAP domain is evolutionarily conserved with sequence homology to GAPs with dual specificity for Ras and Rap GTPases like Syngap1 (Rohm et al., 2000; Wang et al., 2013). There are two conserved catalytic arginine fingers in the Plxn GAP domain that are essential for catalytic activity (Rohm et al., 2000; Wang et al., 2013). The Plxn family member PlxnB1 was initially reported to stimulate the GTPase activity of M-Ras and R-Ras (Oinuma et al., 2004; Saito et al., 2009). However, subsequent structural studies suggest that the GAP domain of Plxns acts as a dimerization-dependent GAP for Rap1 and Rap2 family members (Wang et al., 2012; Wang et al., 2013).

In the mouse, DG development commences around midgestation when neural stem and progenitor cells (NSPCs) are born in the dentate neuroepithelium (Altman and Bayer, 1990). At embryonic day (E)15, NSPCs begin to migrate radially toward the hippocampal fissure (HF), forming a migratory stream into the DG anlage (Li and Pleasure, 2005). Cells in transit include NSPCs and postmitotic immature granule cells (GCs). Upon arrival in the DG, NSPCs form a transient germinative pool with actively dividing cells in the subpial space near the HF (Li et al., 2009). Cell-fate mapping studies revealed that precursor cells in the subpial neurogenic niche transition to the subgranular zone (SGZ) during the first postnatal week (Li et al., 2009) and, together with cells originating from the ventral pole of the hippocampus, populate the SGZ with long-lived neural stem cells (Li et al., 2013). There is functional heterogeneity along the dorsal (septal) and ventral (temporal) axes of the DG; GCs in the dorsal hippocampus participate in spatial and contextual learning, whereas GCs in the ventral hippocampus influence innate anxiety-like behavior (Kheirbek et al., 2013).

Here, we report that select members of the PlxnA family participate in DG morphogenesis and the formation of the SGZ neurogenic niche. PlxnA2 forward signaling through the small GTPase Rap1 is required for proper GC distribution. Behavioral studies with *Plxna2*^{-/-} mice reveal defects in sociability, associative learning, and sensorimotor gating, traits conserved across species and commonly observed in neuropsychiatric disorders.

RESULTS

Plxna2 and *Plxna4* Deficiency Leads to Impaired GC Distribution in the Developing DG

To assess the role of individual PlxnA family members during progenitor cell migration from the dentate neuroepithelium toward the HF (Figure 1A), we analyzed *Plxna1*, *Plxna2*, *Plxna3*, and *Plxna4* mutant mice. Postnatal day (P)1 brains of wild-type (WT) and *Plxna* mutant mice were stained with anti-Prox1, a marker for postmitotic GCs traveling through the dentate migratory stream (DMS) toward the HF to take up residence in the DG anlage (Bagri et al., 2002). At P1 in WT mice, Prox1⁺ cells are found abundantly in the suprapyramidal granule cell layer (CL) (Figure 1B) but rarely in the dentate hilus or DMS. In P1 *Plxna1*^{-/-} (Figure 1C) and *Plxna3*^{-/-} pups (Cheng et al., 2001), distribution of Prox1⁺ cells is comparable to that in WT littermate controls. In marked contrast, *Plxna2*^{-/-} pups show a broad dispersion of Prox1⁺ cells across the emerging dentate field and scattered Prox1 labeling along the DMS (Figure 1D). Compared to P1 WT pups, the *Plxna2*^{-/-} suprapyramidal GCL is shortened, and the infrapyramidal GCL and dentate hilus are densely populated with Prox1⁺ cells (Figure 1D). In *Plxna4*^{-/-} pups, Prox1⁺ progenitors populate the suprapyramidal GCL; however when compared to WT pups, significantly fewer GCs are found near the medial pole of the GCL (Figure 1E). Quantification of these phenotypes revealed that both *Plxna2* and *Plxna4* regulate GC distribution in the DG dorsal blade—however, in distinct manners—resulting either in a decrease or increase of Prox1⁺ cells (Figure 1F).

The prominent expression of PlxnA2 in the developing fore-brain and the association of human *PLXNA2* allelic variants with neuropsychiatric disorders prompted a deeper analysis of PlxnA2 signaling pathways and their role in complex behavior. In particular, DG connectivity with the hippocampus proper is emerging as a target for neuropsychiatric illness (Kobayashi, 2009). Morphological analyses of SCZ brains revealed reduced hippocampal subfield volumes, including reduced size of the DG and impaired mossy fiber-CA3 connectivity (Haukvik et al., 2015; Tamminga et al., 2010). More recent work identified the CA2 hippocampal subfield as a critical hub of sociocognitive memory processing (Alexander et al., 2016; Hitti and Siegelbaum, 2014), providing evidence that defects in hippocampal connectivity contribute to mental illness.

The reduced number of Prox1⁺ cells in the dorsal GCL of *Plxna2*^{-/-} mice is suggestive of impaired cell migration, an idea supported by previous work showing that *Plxna2* regulates cell migration in the developing cerebellum (Renaud et al., 2008). Developmental defects in GC distribution and GCL morphology are not transient in nature. At P30, doublecortin (DCX)-positive immature GCs are confined to the SGZ in *Plxna2*^{+/+} mice. In *Plxna2*^{-/-} littermates, the GCL is severely malformed, and immature GCs show ectopic distribution in the DG molecular layer (Figures 1G–1J). At P40, *Plxna2*^{-/-} mice show variable degrees of GCL deformation, and the length of the GCL is consistently reduced by approximately 15% (Figures S1A–S1D). GCL morphological defects persist in 8-month-old mice (Figures S1E and S1F).

During early hippocampal development, immature GCs travel along a radial glial scaffold toward the HF (Li and Pleasure, 2005; Rickmann et al., 1987). The importance of an intact

glial scaffold is highlighted in mice deficient for *reelin*, its lipoprotein receptors, or downstream effector *Dab1* (Brunne et al., 2013; Weiss et al., 2003). Loss of reelin signaling disrupts the formation of the trans hilar radial glial scaffold and the proper positioning of Cajal-Retzius cells near the HF. This leads to aberrant migration and distribution of GCs within the DG (Förster et al., 2002; Frotscher et al., 2003), a phenotype reminiscent of *Plxna2*^{-/-} mutants. To assess whether *Plxna2* deficiency disrupts the radial glial scaffold, P1 hippocampal sections of *Plxna2*^{+/+} and *Plxna2*^{-/-} littermates were immunostained for glial fibrillary acidic protein (GFAP). In *Dab1*-deficient mice, the horseshoe-shaped arrangement of GFAP⁺ glial processes is disrupted (Förster et al., 2002). However, compared to *Dab1* mutants (Figures S1G–S1I), the radial glial scaffold in *Plxna2*^{+/+} and *Plxna2*^{-/-} mice develops normally (Figures S1G and S1H), and reelin⁺ Cajal-Retzius cells are properly positioned near the HF (Figures S1J and S1K). There is, however, a modest increase in the number of reelin⁺ cells near the medial pole of the GCL in *Plxna2*^{-/-} pups, possibly related to a reduction in the overall size of the mutant DG. Together, these studies show that defects in GC distribution observed in *Plxna2*^{-/-} mice are not secondary to malformation of the radial glial scaffold or altered positioning of Cajal-Retzius cells.

At E16, PlxnA2 staining is observed throughout the telencephalic mantle, except for the ventricular zone (VZ) (Figure S2A). Anti-PlxnA2 stains Prox1⁺ cells in the emerging GCL (Figures S2A–S2D). At P1, robust staining is detected in the DG and CA3-CA1 subfields (Figure S2E). Double-labeling revealed overlap between PlxnA2 and Prox1, but not with GFAP (Figures S2F–S2J). We independently confirmed PlxnA2 expression in GCs and CA3 pyramidal neurons, but not astrocytes, in primary forebrain cultures (Figures S2K–S2M). Specificity of the anti-PlxnA2 antibody was demonstrated by parallel processed brain sections of *Plxna2*^{-/-} pups (Figure S2G).

Reduced Cell Proliferation in the DG of *Plxna2*^{-/-} Mice

To examine whether *Plxna2* deficiency alters DG progenitor cell division, juvenile mice received a single intra-peritoneal (i.p.) injection of bromodeoxyuridine (BrdU), and brains were collected 2 hr later. At P30 and at P14, numerous BrdU⁺ cells are found in the dentate hilus of *Plxna2*^{+/+} mice, the majority of which are confined to the SGZ (Figures 2A and S3A). In parallel processed *Plxna2*^{-/-} littermates, the number of BrdU⁺ cells in the DG is significantly reduced (Figures 2B, 2C, S3B, and S3C). Moreover, in *Plxna2*^{-/-} mice, ectopically positioned BrdU⁺ cells are observed within the dentate molecular layer (Figure S3B). Fewer BrdU⁺ cells suggests that the pool of progenitor cells is reduced, due to either defective migration into the DG or increased death of progenitors after successful migration into the DG. To differentiate between these possibilities, we subjected P14 forebrain tissue sections to TUNEL staining. Labeled cells were readily detected in the neocortex (Figure S3F); however, the DG of neither *Plxna2*^{+/+} nor *Plxna2*^{-/-} mice showed TUNEL⁺ cells (Figures S3D and S3E). Together, these results suggest that decreased germinal activity in the DG of *Plxna2*^{-/-} mice is not secondary to increased cell death. When coupled with the ectopic distribution of BrdU⁺ cells, our data suggest that progenitor cell migration and assembly of the SGZ neurogenic niche require *Plxna2* function.

***Plxna2* Deficiency Perturbs Adult Neurogenesis**

The SGZ stem cell niche reaches maturity around the third postnatal week (Nicola et al., 2015). For selective labeling of dentate progenitor cells and their progeny after the neurogenic niche is assembled, we crossed the *Plxna2* null allele onto an *R26R-YFP; Nestin-CreER^{T2}* background. For cell-fate mapping studies, P30 *R26R-YFP; Nestin-CreER^{T2}* mice and littermate controls were injected with tamoxifen and sacrificed at P60 (Figure 2D). In *Plxna2^{+/+}* and *Plxna2^{+/-}* mice, YFP⁺ cells are abundantly detected in the SGZ and inner GCL, many of which extend apical dendrites into the molecular layer (Figures 2E, 2E', and 2G, and 2G'). Strikingly, in *Plxna2^{-/-}* mice, there is a 77% decrease in YFP⁺ cells (Figures 2F, 2F', and 2I), indicating that loss of *Plxna2* severely impairs adult dentate neurogenesis. To examine whether *Plxna2* is required for neurogenesis after the stem cell niche has formed, we sought to selectively ablate *Plxna2* in nestin⁺ cells after DG development is completed. For inducible ablation of *Plxna2* in nestin⁺ cells, *Plxna2^{flox/-}; R26R-YFP; Nestin-CreER^{T2}* animals were injected with tamoxifen at P30, and brains were collected at P60. In parallel processed *Plxna2^{+/-}* control mice, many YFP⁺ cells were found in the SGZ and GCL (Figures 2G and 2G'); however, inducible deletion of *Plxna2* in NSCs of *Plxna2^{flox/-}; R26R-YFP; Nestin-CreER^{T2}* animals does not lead to a decrease in YFP⁺ cells (Figures 2H, 2H', and 2I). This shows that once the stem cell niche is mature, loss of *Plxna2* no longer impairs neurogenesis.

***Sema5A* Mutant Mice Exhibit Migration Defects Similar to Those Observed in *Plxna2* Mice**

To identify ligands that govern PlxnA2-dependent GC migration, we analyzed the hippocampus of *Sema5A^{-/-}* P1 pups using anti-Prox1 immunolabeling. *Sema5A^{-/-}* pups exhibit defects in the distribution of Prox1⁺ cells, similar to those observed in *Plxna2^{-/-}* mice (Figures 3A–3E). Since *Sema5A* binds directly to PlxnA2 (Duan et al., 2014), our studies suggest that *Sema5A* functions as PlxnA2 ligand in the developing DG. To explore *Sema5A*-PlxnA2 downstream signaling mechanisms, we focused on the PlxnA2 GAP domain and tested the role of small GTPases using the collapse of transiently transfected COS7 fibroblasts as a model system. In COS7 cells, WT PlxnA2, but not a GAP-activity-deficient PlxnA2, triggers rapid cytoskeletal collapse in the presence of bath-applied *Sema5A*-Fc (Figures 3F and 3G), demonstrating a critical role of the GAP domain in cell collapse (Duan et al., 2014). Multiple lines of evidence show that Plxns function as GAPs for Ras/Rap family GTPases (Püschel, 2007; Wang et al., 2012). Rap family GTPases, including Rap1A, Rap1B, and Rap2 control cell shape (Dao et al., 2009) and are regulated by PlxnA family members *in vitro* (Yoo et al., 2016). We find that the small GTPase Rap1B is required for *Sema5A*-PlxnA2 signaling, since co-transfection of the constitutively active mutant Rap1B(Q63E) stimulates spreading of PlxnA2⁺ COS7 cells in the presence of bath-applied *Sema5A*-Fc (Figures 3I and 3J). Co-expression of PlxnA2 and WT Rap1B does not attenuate *Sema5A*-Fc-elicited cytoskeletal collapse (Figures 3H and 3J). These observations suggest that PlxnA2 is a negative regulator of the GTPase Rap1B.

***Rap1* Regulates GC Distribution in the Developing DG**

Next, we asked whether *Rap1* deficiency mimics the GC migration defects observed in the *Sema5A^{-/-}* and *Plxna2^{-/-}* mutants. Global deletion of both Rap1 isoforms, *Rap1a* and

Rap1b, is embryonically lethal (Chrzanowska-Wodnicka et al., 2015). Conditional ablation of *Rap1a* and *Rap1b* in the developing mouse nervous system identified Rap1 GTPases as key regulators of cell polarity (Shah et al., 2017). Rap1 GTPases regulate the polarization of radial glia cells and are required for the formation of leading processes of multipolar neurons and also their migration toward the cortical plate (Jossin and Cooper, 2011; Shah et al., 2017). Because Rap1 GTPases function in the polarization of radial glia and neurons, we used mice that lack *Rap1* selectively in neurons: *Rap1a^{flox/flox};Rap1b^{flox/flox};Nex-cre*, hereinafter called *Rap1;Nexcre* (Shah et al., 2017). At P1, anti-Prox1 staining of *Rap1;Nexcre* conditional brains revealed fewer GCs within the dorsal blade of the DG anlage (Figures 3K–3O), reminiscent of *Sema5A^{-/-}* and *Plxna2^{-/-}* mice. When coupled with the observation that Rap1B inhibition is required for PlxnA2-mediated COS7 collapse, our studies suggest that PlxnA2 regulates GC migration in a Rap1-dependent manner.

PlxnA2 GAP Activity Is Required for GC Migration but Not for Neurogenesis

To directly test whether PlxnA2 GAP activity is required for proper GC distribution, we used CRISPR/Cas9 gene editing to replace the catalytically important arginine 1746 in the PlxnA2 GAP domain with alanine, resulting in the mutant allele *Plxna2^{R1746A}* (Figure S4A). Mice homozygous for the *R1746A* point mutation (hereinafter referred to as *Plxna2^{R/R}*) are born at the predicted Mendelian ratios and viable into adulthood (data not shown). To assess PlxnA2 production and distribution in *Plxna2^{R/R}* mice, P1 forebrain sections of *Plxna2^{+/+}* and *Plxna2^{R/R}* mice were subjected to anti-PlxnA2 staining, revealing similar labeling patterns (Figures S4E and S4F). Immunoblotting of forebrain cell culture lysates (Figures 4A and 4C) or whole brain lysates (Figures S4B and S4C) showed comparable levels of PlxnA2 in *Plxna2^{+/+}*, *Plxna2^{R/R}*, and *Plxna2^{+/-}* mice. Primary neurons prepared from *Plxna2^{+/+}* and *Plxna2^{R/R}* embryos show surface localization of PlxnA2 (Figures 4B and 4C) and strongly support the binding of bath-applied Sema5A-Fc, while binding to *Plxna2^{-/-}* primary neuronal cultures processed in parallel is significantly reduced (Figure S4D). As a control, we show that NgR^{OMNI}-Fc, a soluble variant of the Nogo66 receptor 1, strongly binds to primary neurons, independent of *Plxna2* genotype (Figure S4D). Based on these observations, we conclude that *Plxna2^{R1746A}* is expressed at levels comparable to WT PlxnA2, localized to the neuronal cell surface, and supports Sema5A binding similar to WT PlxnA2.

Analysis of the hippocampus of *Plxna2^{R/R}* P1 pups revealed defects in Prox1⁺ cell distribution in the DG (Figures 4D and 4E). Similar to *Plxna2^{-/-}* mice, *Plxna2^{R/R}* pups show more Prox1⁺ cells within the hilus. In more mature *Plxna2^{R/R}* mice, defects in GCL morphology are observed (Figures S4J and S4K), but they are less pronounced than in *Plxna2^{-/-}* mice (Figure S1). To assess cell proliferation, P30 *Plxna2^{R/R}* mice received a single injection of BrdU, and brains were collected after 2 hr. The number of BrdU⁺ cells in the DG of *Plxna2^{R/R}* mice is comparable to that in *Plxna2^{+/+}* littermates, indicating that the PlxnA2 GAP domain is not required for dentate neurogenesis (Figures S4G–S4I).

PlxnA2 GAP Activity Is Dispensable for Mossy Fiber-CA3 Targeting

GC axons, called mossy fibers, project through the hilus and to the CA3 stratum pyramidale in the form of a large suprapyramidal tract (SPT) and a smaller infrapyramidal tract (IPT).

Mossy fibers form large presynaptic specializations, the mossy fiber boutons (MFBs), to establish synaptic connectivity with the apical and basal dendrites of CA3 pyramidal neurons. Previous work established a critical role for *Plxna2* in mossy-fiber patterning and the distribution of MFBs within CA3 (Suto et al., 2007; Tawarayama et al., 2010). To assess whether the PlxnA2 GAP activity is required for proper mossy-fiber targeting and MFB distribution, the brains of *Plxna2*^{+/+}, *Plxna2*^{-/-}, and *Plxna2*^{R/R} mice were subjected to anti-calbindin labeling and also Timm's silver sulfide staining to visualize presynaptic zinc. For selective labeling of MFBs, anti-synaptopodin (SPO) and anti-vesicular glutamate transporter 1 (vGLUT1) double-immunofluorescence labeling was used (Williams et al., 2011). Consistent with Suto et al. (2007), mossy-fiber patterning is defective in *Plxna2*^{-/-} mice, since axons in the SPT fail to properly innervate the stratum lucidum but, instead, innervate the strata pyramidale and oriens (Figures 5 and S5). Strikingly, in *Plxna2*^{R/R} mice, mossy-fiber patterning is largely intact. The majority of axons in the SPT are confined to the stratum lucidum, with only a few calbindin⁺ axonal sprouts entering the CA3 stratum pyramidale (Figure S5C). Moreover, the majority of vGLUT1- and SPO-stained MFBs properly formed in the stratum lucidum (Figure 5C). This finding was independently confirmed by Timm's staining of *Plxna2*^{R/R} mice (Figure S5). Collectively, our studies show that the PlxnA2 GAP activity is dispensable for mossy fiber-CA3 targeting and the formation of MFB in the stratum lucidum.

Morphological Defects in the Hippocampus of Adult *Plxna2*^{-/-} Mice Do Not Result in Epileptiform Activities

Ectopic positioning of GCs and malformation of the DG are frequently observed in temporal lobe epilepsy. For example, *NeuroD1* mutant mice exhibit malformation of the DG and show spontaneous seizures (Liu et al., 2000). Dispersion of GCs is also observed in *reelin*- and *Dab1*-deficient mice (Brunne et al., 2013; Weiss et al., 2003) and is epileptogenic (Korn et al., 2016). Further, spontaneous seizures have been reported for Sema and Sema receptor knockout mice, some of which exhibit aberrant hippocampal connectivity (Gant et al., 2009; Sahay et al., 2005). To assess whether *Plxna2* mice are epileptic, we performed long-term video EEG (electroencephalogram) monitoring from epidural scalp electrodes of adult *Plxna2*^{-/-}, *Plxna2*^{+/-}, and WT mice. Despite defects in GCL morphology and mossy fiber-CA3 connectivity, *Plxna2*^{-/-} mice show normal EEGs (Figure S6A). No spontaneous seizures or interictal epileptiform discharges were observed over a ten-day recording period, suggesting that morphological abnormalities in *Plxna2*^{-/-} mice are not epileptogenic.

***Plxna2*^{-/-} Mice Show Reduced Anxiety**

Although adult *Plxna2*^{-/-} mice show abnormalities in brain architecture, the impact on behavior has not yet been examined. Given the previously reported association among *PLXNA2* and *SEMA5A* allelic variants and neuropsychiatric disorders (Charney et al., 2017; Kirov, 2015; Schizophrenia Working Group of the Psychiatric Genomics Consortium, 2014), we subjected *Plxna2* mice to a battery of behavioral tests with relevance to psychiatric disorders. In the open field test (OFT), *Plxna2*^{+/+}, *Plxna2*^{+/-}, and *Plxna2*^{-/-} mice show normal locomotor levels and the same total distance traveled (Figure 6A). WT mice exhibit an innate aversion to bright open spaces and avoid the center zone of the OFT chamber. Time spent in the center zone is inversely related to anxiety levels. Compared to

Plxna2^{+/+} and *Plxna2*^{+/-} mice, the distance traveled in the center zone by *Plxna2*^{-/-} is significantly greater. This suggests that *Plxna2*^{-/-} mice exhibit reduced anxiety-like behavior (Figure 6B).

Fear Memory Is Altered in *Plxna2*^{-/-} Mice

Pavlovian fear conditioning provides a measure of associative memory. Mice quickly learn to predict an aversive event, such as a mild foot shock, in association with a particular (neutral) context or auditory stimulus. Prior to the first tone-shock pairing on day 1 of training, *Plxna2*^{+/+}, *Plxna2*^{+/-}, and *Plxna2*^{-/-} mice did not exhibit significant freezing. Although all genotypes showed significant increases in freezing as training progressed, *Plxna2*^{-/-} mice exhibited significantly less freezing than *Plxna2*^{+/+} and *Plxna2*^{+/-} mice (Figure 6C). Twenty-four hours after the completion of training, animals were exposed to the context in the absence of a shock or tone. *Plxna2*^{-/-} mice exhibited significantly less freezing to the context than their *Plxna2*^{+/+} and *Plxna2*^{+/-} littermates (Figure 6D). Twenty-four hours after the context test, cued conditioning was assessed in a reconfigured context. Freezing increased significantly for all groups after presentation of the tone, but *Plxna2*^{-/-} mice froze significantly less than their littermates both at baseline and during tone presentation (Figure 6E). However, there was no genotype-tone interaction, $F(1, 47) = 2.415$, $p = 0.1$, repeated-measures ANOVA; and there was no significant difference in pre-tone freezing levels, $F(2, 47) = 2.415$, $p = 0.09$, one-way ANOVA. These results suggest that the lower levels of freezing observed in the *Plxna2*^{-/-} mice during the cued testing likely reflects a deficit in fear generalization. Unlike the WT mice, the *Plxna2*^{-/-} mice exhibit less freezing when introduced to the novel chamber because they failed to properly consolidate the original training context. No differences between *Plxna2*^{-/-} males and females were detected (data not shown). In sum, fear conditioning experiments indicate that *Plxna2*^{-/-} mice exhibit defects in contextual fear memory but not in cued fear memory.

Plxna2^{-/-} Females, but Not Males, Show Impaired Sociability

Next, *Plxna2* mice were assayed in the three-chambered apparatus, a simple social approach test (Yang et al., 2011). *Plxna2*^{+/+}, *Plxna2*^{+/-}, and *Plxna2*^{-/-} mice spent significantly more time engaged in nose-to-nose interaction with a WT C57BL/6 mouse than in sniffing an inanimate object (Figures 6F and S6B), a behavior representing normal sociability (Roullet and Crawley, 2011). We next assessed the time of direct nose-to-nose interaction of *Plxna2*^{+/+}, *Plxna2*^{+/-}, and *Plxna2*^{-/-} mice with a novel versus a familiar WT C57BL/6 mouse. The time spent with a novel mouse was significantly greater for all three genotypes. As sex is an important variable in this assay (Beery and Kaufer, 2015), we separated tested male and female mice. Female *Plxna2*^{+/+} and *Plxna2*^{+/-} mice show a strong preference for nose-to-nose contact with the novel female mouse; however, female *Plxna2*^{-/-} mice do not, suggesting impaired sociability (Figure 6G). This stands in contrast to male mice, as they show a strong preference for the novel male mouse, independent of *Plxna2* genotype (Figure 6G). In addition, when the same data were analyzed using a discrimination ratio as the dependent variable, all groups performed above chance, except the female *Plxna2*^{-/-} mice (Figure S6C). These data suggest that *Plxna2* deficiency disrupts social behavior in female, but not male, mice.

***Plxna2* Deficiency Causes Impaired Sensorimotor Gating**

Sensorimotor gating, or the ability of a sensory event to suppress a motor response, can be measured operationally via prepulse inhibition (PPI) of the acoustic startle response (Powell et al., 2012). PPI is deficient in SCZ patients and in some other neuropsychiatric disorders and can be measured across different species (Powell et al., 2012; Swerdlow et al., 2008). In an effort to mimic the PPI testing conditions used in patient studies, we recorded PPI using an established protocol with minimal background noise (Renoux et al., 2014). The startle response to a brief loud sound (20 ms, 120 dB) or the response to “analog” (quiet trial, no auditory stimulation) was analyzed. There were no *Plxna2* genotype- or sex-dependent differences in the startle magnitude among the three genotypes (Figures 7A and 7C). When the 120-dB startle sound was preceded by a brief acoustic stimulus at different sound intensities (40, 50, and 65 dB), delivered as either narrowband (12 kHz) or broadband noise (BBN), the startle response was significantly suppressed in *Plxna2*^{+/+} male and female mice. In *Plxna2*^{+/-} males, but not females, PPI is significantly reduced, compared to *Plxna2*^{+/+} mice (Figures 7B and 7D). PPI in *Plxna2*^{-/-} male and female mice is significantly reduced if the prepulse is provided at 40, 50, and 65 dB, as narrowband or as BBN (Figures 7B and 7D). To rule out impaired hearing in *Plxna2*^{-/-} mice as a potential confounding effect, mice were subjected to a sensitive hearing test and found to be normal (Figures S6D and S6E). Collectively, these studies show that sensorimotor gating is impaired in a *Plxna2* gene-dosage- and sex-dependent manner.

PlxnA2 GAP Activity Is Required for Contextual Fear Conditioning and PPI

Since *Plxna2*^{R/R} mice show greatly reduced morphological defects when compared to *Plxna2*^{-/-} mice, we asked whether *Plxna2*^{-/-} behavioral defects persist in *Plxna2*^{R/R} mice. The anxiolytic phenotype observed in the OFT of *Plxna2*^{-/-} mice is no longer observed in *Plxna2*^{R/R} mice (Figures 6B, S7A, and S7B). However, when tested for fear memory, *Plxna2*^{R/R} mice show defects in contextual fear conditioning but not cued fear conditioning (Figures S7C–S7E); in essence, phenocopying defects observed in *Plxna2*^{-/-} mice (Figures 6C–6E). This shows that defects in GCL morphogenesis and mossy fiber-CA3 targeting in *Plxna2*^{-/-} mice are not causally linked to defects in contextual fear memory.

To assess whether the PlxnA2 GAP activity is important for PPI, we analyzed adult *Plxna2*^{+/+}, *Plxna2*^{R/+}, and *Plxna2*^{R/R} mice. The startle amplitude to a sharp 120-dB sound is very similar among all three genotypes (Figure 7E), in both males and females (Figures S8A and S8C). PPI in *Plxna2*^{R/+} is comparable to that in *Plxna2*^{+/+} mice when the prepulse is provided at different sound intensities (40, 50, and 65 dB) delivered either as narrowband or BBN (Figures 7F, S8B, and S8D). In marked contrast, *Plxna2*^{R/R} mice exhibit impaired PPI at 40, 50, and 65 dB, provided as narrowband and BBN (Figure 7F). Moreover, there are sex-dependent differences in PPI for PlxnA2 GAP-deficient mice. Male *Plxna2*^{R/R} mice show a more pronounced PPI phenotype than their littermate *Plxna2*^{R/R} females (Figure S8). In sum, these studies show that PlxnA2 GAP forward signaling is critical for normal sensorimotor gating.

DISCUSSION

Here, we report on a mechanism that controls DG development *in vivo*. We show that *Sema-PlxnA* signaling regulates the distribution of immature GCs in the DG anlage. Similar to the *Reeler* mouse, migration of GCs into the DG is apparently stalled in *Plxna2*^{-/-} mice. Reelin is important for the formation of the glial scaffolding along which GCs travel. In *Plxna2*^{-/-} mice, the glial scaffolding develops normally, and the distribution of reelin is comparable to that in *Plxna2*^{+/+} mice. A cell-autonomous function for *Plxna2* in GC migration is supported by the observations that loss of GAP activity or neuron-specific ablation of *Rap1* each result in aberrant GC distribution. In its active form, Rap1 increases integrin activation and promotes cell adhesion (Dao et al., 2009; Kim et al., 2011). Similar to *PlxnA2*, *CXCL12* signaling through the chemokine receptor *CXCR4* is critical for GC migration (Bagri et al., 2002). In lymphocytes, *CXCL12/CXCR4* signaling regulates chemoattraction through Rap1 and subsequent reduction of integrin adhesion (Shimonaka et al., 2003). Interestingly, *Sema3A*-mediated chemorepulsion of sensory neurons is mitigated by *CXCL12* (Chalasan et al., 2003), suggesting that *PlxnA* and *CXCR4* share common downstream signaling mechanisms. We propose that GC migration and distribution in the developing DG is controlled by *Sema/PlxnA*- and *CXCL12/CXCR4*-dependent regulation of Rap1 activity and inside-out integrin activation.

PlxnA2 Regulates GCL Morphogenesis

We previously reported that *Sema5A* and *Sema5B* bind to *PlxnA2* directly (Duan et al., 2014); here, we show that *Sema5A*^{-/-} pups exhibit defects in GC distribution similar to those in *Plxna2*^{-/-} mutants. However, in adult *Sema5* single and *Sema5A*^{-/-};*Sema5B*^{-/-} double mutants, the GCL appears normal (Duan et al., 2014). This suggests that additional *PlxnA2* ligands participate in GCL morphogenesis. *Sema6A* and *Sema6B* associate with *PlxnA2* (Perez-Branguli et al., 2016; Suto et al., 2007). Interestingly, mice deficient for *Sema6A*^{-/-} show mild but consistent malformation of the lower blade of the GCL and ectopic positioned GCs in the dentate molecular layer (Rünker et al., 2011). This suggests that, in addition to *Sema5A*, *Sema6A-PlxnA2* signaling contributes to GCL morphogenesis. Dentate development and adult GCL morphology in *Sema6A*^{-/-};*Sema6B*^{-/-} or *Sema5/Sema6* compound mice has not yet been examined, and additional studies are needed to identify the full spectrum of *PlxnA2*-dependent signaling events that underlie GCL morphogenesis.

PlxnA2 GAP Activity Is Not Required for Mossy Fiber Laminal Targeting

Plxna2 is required for proper targeting of the mossy fiber SPT within the stratum lucidum and IPT within the stratum oriens of CA3 (Suto et al., 2007). Analysis of *Plxna2*^{R/R} mice revealed that the GAP domain is dispensable for mossy fiber laminal targeting. *PlxnA2* supports the binding of *Sema5A* and *Sema5B*; however, neither *Sema5* single mutants nor *Sema5A*^{-/-};*Sema5B*^{-/-} double mutants show defects in mossy fiber targeting (Duan et al., 2014). Aberrant SPT and IPT patterning is observed in *Sema6A*^{-/-}/*Sema6B*^{-/-} double mutants, although defects are comparatively mild and distinct from those in *Plxna2*^{-/-} mice (Suto et al., 2007; Tawarayama et al., 2010). Interestingly, mossy fiber defects in *Plxna2*^{-/-} mice are no longer observed in *Plxna2*^{-/-};*Sema6A*^{-/-} and *Plxna2*^{-/-};*Sema6B*^{-/-} compound

mutants, showing that *Sema6A* and *Sema6B* are epistatic to *Plxna2* (Suto et al., 2007; Tawarayama et al., 2010). This suggests that, in *Plxna2*^{-/-} mice, aberrant mossy fiber invasion of the CA3 stratum pyramidale is a result of increased Sema6 repulsion. Loss of Sema6 association with PlxnA2 in *cis* has been proposed to enhance Sema6 repulsion through PlxnA4 in *trans* (Battistini and Tamagnone, 2016). In support of this idea, *cis* association between PlxnA2 and transmembrane Semas has been shown to attenuate signaling in *trans* (Duan et al., 2014; Perez-Branguli et al., 2016). Sema6A and Sema6B are found along dendrites of hippocampal pyramidal neurons (Suto et al., 2007; Tawarayama et al., 2010). When coupled with the presence of PlxnA2 on dendrites of cultured CA3 pyramidal neurons (Figure S2) and PlxnA4 on mossy fibers (Suto et al., 2007), this suggests that Sema6 repulsion is tempered by PlxnA2 association in *cis*, thereby enabling mossy fiber innervation of the stratum lucidum. This model is consistent with our observation that PlxnA2 GAP activity is not required for mossy fiber patterning and suggests that PlxnA2 does not function as a canonical Sema receptor but, rather, as a *cis* inhibitor of Sema6, gauging repulsion toward developing mossy fibers.

Morphological Defects in the Hippocampus of *Plxna2* Mice Can Be Dissociated from Behavioral Defects

It is well appreciated that Pavlovian fear conditioning in rodents requires an intact amygdala and contextual fear memory additionally requires a functionally intact hippocampus (Kim et al., 1992; Maren, 2001). *Plxna2*^{-/-} mice exhibit deficits in Pavlovian fear conditioning, especially when context is used as the conditioned stimulus. It is worth noting here that the *Plxna2*^{-/-} mice also exhibit less freezing in general during testing with a tone conditional stimulus (CS) (both before and during presentation of the tone). This behavior does not appear to be due to hyperactivity, as the *Plxna2*^{-/-} mice exhibit similar levels of locomotor activity in the open field. Rather, the lower levels of freezing may reflect a lower level of basal anxiety, given that the *Plxna2*^{-/-} mice tended to spend significantly more time in the center of the open field, which is often suggestive of an anxiolytic state. Unlike in *Plxna2*^{-/-} mice, no change in anxiolytic state is observed in PlxnA2 GAP-deficient mice, yet these mice also show defects in contextual fear memory but not cued fear memory. This shows that, in *Plxna2*^{-/-} mice, impaired fear memory is likely not causally linked to an anxiolytic state.

In *Plxna2*^{-/-} mice, but not *Plxna2*^{R/R} mice, the GCL is malformed, mossy fiber laminar targeting is defective, and adult neurogenesis is impaired, yet both *Plxna2*^{-/-} and *Plxna2*^{R/R} mice exhibit deficits in contextual fear memory and PPI. This shows that morphological defects in the hippocampus of *Plxna2*^{-/-} mice are not causally linked to behavioral defects. This begs the question of what is the underlying neural substrate. Subtle morphological defects persist in the DG-CA3 connectivity of *Plxna2*^{R/R} mice and may cause behavioral defects. Alternatively, PlxnA2 GAP activity may regulate GC synaptic inputs from the entorhinal cortex, contralateral hippocampus, mossy cells, feedback from CA3, or neuromodulatory neurons and thereby impair DG function in *Plxna2*^{R/R} mice (Gonçalves et al., 2016). Previous studies showed that Sema-PlxnA signaling can influence GC synaptic density and strength (Duan et al., 2014; Tran et al., 2009) and that loss of PlxnA2 GAP may perturb synaptic function and cause behavioral defects. Given the broad expression of

PlxnA2 in the developing nervous system, it is entirely possible that neural ensembles outside the hippocampus underlie defects in fear memory, sociability, and sensorimotor gating. Additional studies will be needed to define brain regions and neural circuits that require *Plxna2* function to ensure normal behavior.

Sema/PlxnA2 Forward Signaling and Mental Health

In mice, loss of the PlxnA2 ligands *Sema5A* and *Sema6A* leads to behavioral deficits suggestive of mental illness. *Sema5A*^{-/-} mice show reduced sociability but no changes in anxiety levels or defects in fear memory (Duan et al., 2014). *Sema6A*^{-/-} mice exhibit deficits in object recognition and working memory, as well as altered social interaction. Moreover, anxiety levels in *Sema6A*^{-/-} males, but not females, are reduced (Rünker et al., 2011). These behavioral phenotypes are partially replicated in *Plxna2*^{-/-} mice, but there are also clear differences; *Plxna2*^{-/-} males and females show an anxiolytic phenotype, and sociability is selectively impaired in females but not in males.

Genome-wide association studies (GWASs) of case/control cohorts found a significant association between SNPs in *PLXNA2* and schizophrenics with European, European-American, or Latin-American descent (Mah et al., 2006). Follow-up studies expanded these findings to a Japanese population (Takeshita et al., 2008), but studies with additional subjects found no significant association between SNPs in *PLXNA2* and SCZ in a Japanese population (Fujii et al., 2007) or Chinese population (Budel et al., 2008). This suggests that, in different populations, *PLXNA2* confers varying genetic risk to SCZ. Expression of *PLXNA2* was shown to associate with *cis* SNPs in the frontal cortex, but not hippocampus, in SCZ patients aged 25–62 years (Kim et al., 2012). Independent studies reported association between *PLXNA2* SNPs and anxiety, neuroticism, and psychological distress (Coric et al., 2010; Wray et al., 2007).

In addition to *PLXNA2*, mutations in *SEMA5A* (Mosca-Boidron et al., 2016; Weiss et al., 2009), *RAP1* (Stornetta and Zhu, 2011), and *CXCL12/CXCR4* (Toritsuka et al., 2013) associate with increased risk for neuropsychiatric illness. Of interest, the scaffold protein Shank3 negatively regulates integrin-mediated cell adhesion by binding Rap1 and, thereby, sequestering it away from the plasma membrane (Lilja et al., 2017). Thus, similar to PlxnA2 GAP activity, Shank3 inhibits Rap1 GTPases. Notably, the autism-associated mutations SHANK3(L68P) and SHANK3(R12C) fail to inhibit Rap1 (Lilja et al., 2017), suggesting a functional link between Shank3 and PlxnA2 in reducing Rap1 activity and integrin activation. Conversely, dysregulation of Rap GTPases, as a result of impaired Rap GEF activity, can have detrimental effects on mental health (Bithell et al., 2010; Stornetta and Zhu, 2011). Taken together, our studies suggest that mutations in *PLXNA2*, and gene products that influence *PLXNA2* forward signaling and *RAP1* activity, contribute to neuropsychiatric illness.

EXPERIMENTAL PROCEDURES

Animals

All procedures involving mice were approved by the University of Michigan Institutional Animal Care and Use Committee and performed in accordance with guidelines developed by the NIH. *Plxna2*^{-/-}, *Sema5A*^{-/-}, and *Plxna2*^{flox/flox} mice have been described previously (Duan et al., 2014; Sun et al., 2013). *Plxna2(R1746A)* mice were generated by the University of Rochester Mouse Genome Editing Resource, using CRISPR/Cas9. For details, see the Supplemental Information.

Histological Procedures

Animal perfusion, tissue preparation, and staining were carried out as described previously (Duan et al., 2014). For BrdU labeling of dividing cells, mouse pups at P14 and P30 were injected with a single dose of BrdU 2 hr before brains were collected. Distribution of Prox1⁺ cells in the DG was assessed in P1 brain sections using ImageJ.

Behavioral Studies

Cohorts of adult WT and mutant male and female mice on a C57BL/6 background were used to assess locomotion, anxiety, fear memory, sociability, and sensorimotor gating using established protocols.

Statistical Analysis

GraphPad Prism 7 was used for data analysis. A two-tailed unpaired Student's t test was used for single comparison. One-way, two-way, and repeated-measures ANOVAs were performed for multiple comparisons. Details on statistical analyses are provided in the figure legends. $p < 0.05$ was considered statistically significant. Details on "n" representation and exact value are included in the figure legends.

Supplementary Material

Refer to Web version on PubMed Central for supplementary material.

Acknowledgments

We thank Drs. Amar Sahay, Sue O'Shea, Alain Chédotal, and Alex Kolodkin and members of the Giger laboratory for critical reading and commenting on the manuscript. We thank Dr. Xuewu Zhang for sharing the Rap1 plasmids. This work was supported by NIH grants P30 DC05188 (to D.F.D.), R01 NS058585 (to J.M.P.), and R01 NS081281 (to R.J.G.); the Deutsche Forschungsgemeinschaft (DFG) through the Cells-in-Motion Cluster of Excellence (EXC 1003 - CiM) (to J.J. and A.W.P.); a Rackham International Student Fellowship (to R.K.); and the Dr. Miriam and Sheldon G. Adelson Medical Foundation on Neural Repair and Rehabilitation (to R.J.G.).

References

- Alexander GM, Farris S, Pirone JR, Zheng C, Colgin LL, Dudek SM. Social and novel contexts modify hippocampal CA2 representations of space. *Nat. Commun.* 2016; 7:10300. [PubMed: 26806606]
- Altman J, Bayer SA. Migration and distribution of two populations of hippocampal granule cell precursors during the perinatal and postnatal periods. *J. Comp. Neurol.* 1990; 301:365–381. [PubMed: 2262596]

- Bagri A, Gurney T, He X, Zou YR, Littman DR, Tessier-Lavigne M, Pleasure SJ. The chemokine SDF1 regulates migration of dentate granule cells. *Development*. 2002; 129:4249–4260. [PubMed: 12183377]
- Battistini C, Tamagnone L. Transmembrane semaphorins, forward and reverse signaling: have a look both ways. *Cell. Mol. Life Sci*. 2016; 73:1609–1622. [PubMed: 26794845]
- Beery AK, Kaufer D. Stress, social behavior, and resilience: insights from rodents. *Neurobiol. Stress*. 2015; 1:116–127. [PubMed: 25562050]
- Bithell A, Hsu T, Kandaneeratchi A, Landau S, Everall IP, Tsuang MT, Chana G, Williams BP. Expression of the Rap1 guanine nucleotide exchange factor, MR-GEF, is altered in individuals with bipolar disorder. *PLoS ONE*. 2010; 5:e10392. [PubMed: 20436929]
- Brunne B, Franco S, Bouché E, Herz J, Howell BW, Pahle J, Müller U, May P, Frotscher M, Bock HH. Role of the postnatal radial glial scaffold for the development of the dentate gyrus as revealed by Reelin signaling mutant mice. *Glia*. 2013; 61:1347–1363. [PubMed: 23828756]
- Budel S, Shim SO, Feng Z, Zhao H, Hisama F, Strittmatter SM. No association between schizophrenia and polymorphisms of the PlexinA2 gene in Chinese Han Trios. *Schizophr. Res*. 2008; 99:365–366. [PubMed: 18096369]
- Chalasanani SH, Sabelko KA, Sunshine MJ, Littman DR, Raper JA. A chemokine, SDF-1, reduces the effectiveness of multiple axonal repellents and is required for normal axon pathfinding. *J. Neurosci*. 2003; 23:1360–1371. [PubMed: 12598624]
- Chang S, Fang K, Zhang K, Wang J. Network-based analysis of schizophrenia genome-wide association data to detect the joint functional association signals. *PLoS ONE*. 2015; 10:e0133404. [PubMed: 26193471]
- Charney AW, Ruderfer DM, Stahl EA, Moran JL, Chambert K, Belliveau RA, Forty L, Gordon-Smith K, Di Florio A, Lee PH, et al. Evidence for genetic heterogeneity between clinical subtypes of bipolar disorder. *Transl. Psychiatry*. 2017; 7:e993. [PubMed: 28072414]
- Cheng HJ, Bagri A, Yaron A, Stein E, Pleasure SJ, Tessier-Lavigne M. Plexin-A3 mediates semaphorin signaling and regulates the development of hippocampal axonal projections. *Neuron*. 2001; 32:249–263. [PubMed: 11683995]
- Chranowska-Wodnicka M, White GC 2nd, Quilliam LA, Whitehead KJ. Small GTPase Rap1 is essential for mouse development and formation of functional vasculature. *PLoS ONE*. 2015; 10:e0145689. [PubMed: 26714318]
- Coric V, Feldman HH, Oren DA, Shekhar A, Pultz J, Dockens RC, Wu X, Gentile KA, Huang SP, Emison E, et al. Multicenter, randomized, double-blind, active comparator and placebo-controlled trial of a corticotropin-releasing factor receptor-1 antagonist in generalized anxiety disorder. *Depress. Anxiety*. 2010; 27:417–425. [PubMed: 20455246]
- Dao VT, Dupuy AG, Gavet O, Caron E, de Gunzburg J. Dynamic changes in Rap1 activity are required for cell retraction and spreading during mitosis. *J. Cell Sci*. 2009; 122:2996–3004. [PubMed: 19638416]
- Duan Y, Wang SH, Song J, Mironova Y, Ming GL, Kolodkin AL, Giger RJ. Semaphorin 5A inhibits synaptogenesis in early postnatal-and adult-born hippocampal dentate granule cells. *eLife*. 2014; 3:e04390.
- English JA, Pennington K, Dunn MJ, Cotter DR. The neuroproteomics of schizophrenia. *Biol. Psychiatry*. 2011; 69:163–172. [PubMed: 20887976]
- Förster E, Tielsch A, Saum B, Weiss KH, Johanssen C, Graus-Porta D, Müller U, Frotscher M. Reelin, Disabled 1, and beta 1 integrins are required for the formation of the radial glial scaffold in the hippocampus. *Proc. Natl. Acad. Sci. USA*. 2002; 99:13178–13183. [PubMed: 12244214]
- Frotscher M, Haas CA, Förster E. Reelin controls granule cell migration in the dentate gyrus by acting on the radial glial scaffold. *Cereb. Cortex*. 2003; 13:634–640. [PubMed: 12764039]
- Fujii T, Iijima Y, Kondo H, Shizuno T, Hori H, Nakabayashi T, Arima K, Saitoh O, Kunugi H. Failure to confirm an association between the PLXNA2 gene and schizophrenia in a Japanese population. *Prog. Neuropsychopharmacol. Biol. Psychiatry*. 2007; 31:873–877. [PubMed: 17346868]
- Gant JC, Thibault O, Blalock EM, Yang J, Bachstetter A, Kotick J, Schauwecker PE, Hauser KF, Smith GM, Mervis R, et al. Decreased number of interneurons and increased seizures in neuropilin

2 deficient mice: implications for autism and epilepsy. *Epilepsia*. 2009; 50:629–645. [PubMed: 18657176]

- Gonçalves JT, Schafer ST, Gage FH. Adult neurogenesis in the hippocampus: from stem cells to behavior. *Cell*. 2016; 167:897–914. [PubMed: 27814520]
- Haukvik UK, Westlye LT, Mørch-Johnsen L, Jørgensen KN, Lange EH, Dale AM, Melle I, Andreassen OA, Agartz I. In vivo hippocampal subfield volumes in schizophrenia and bipolar disorder. *Biol. Psychiatry*. 2015; 77:581–588. [PubMed: 25127742]
- Henriksen MG, Nordgaard J, Jansson LB. Genetics of schizophrenia: overview of methods, findings and limitations. *Front. Hum. Neurosci*. 2017; 11:322. [PubMed: 28690503]
- Hitti FL, Siegelbaum SA. The hippocampal CA2 region is essential for social memory. *Nature*. 2014; 508:88–92. [PubMed: 24572357]
- Jossin Y, Cooper JA. Reelin, Rap1 and N-cadherin orient the migration of multipolar neurons in the developing neocortex. *Nat. Neurosci*. 2011; 14:697–703. [PubMed: 21516100]
- Kheirbek MA, Drew LJ, Burghardt NS, Costantini DO, Tannenholz L, Ahmari SE, Zeng H, Fenton AA, Hen R. Differential control of learning and anxiety along the dorsoventral axis of the dentate gyrus. *Neuron*. 2013; 77:955–968. [PubMed: 23473324]
- Kim JJ, Fanselow MS, DeCola JP, Landeira-Fernandez J. Selective impairment of long-term but not short-term conditional fear by the N-methyl-D-aspartate antagonist APV. *Behav. Neurosci*. 1992; 106:591–596. [PubMed: 1354443]
- Kim C, Ye F, Ginsberg MH. Regulation of integrin activation. *Annu. Rev. Cell Dev. Biol*. 2011; 27:321–345. [PubMed: 21663444]
- Kim S, Cho H, Lee D, Webster MJ. Association between SNPs and gene expression in multiple regions of the human brain. *Transl. Psychiatry*. 2012; 2:e113. [PubMed: 22832957]
- Kirov G. CNVs in neuropsychiatric disorders. *Hum. Mol. Genet*. 2015; 24(R1):R45–R49. [PubMed: 26130694]
- Kobayashi K. Targeting the hippocampal mossy fiber synapse for the treatment of psychiatric disorders. *Mol. Neurobiol*. 2009; 39:24–36. [PubMed: 19130314]
- Kong Y, Janssen BJ, Malinauskas T, Vangoor VR, Coles CH, Kaufmann R, Ni T, Gilbert RJ, Padilla-Parra S, Pasterkamp RJ, Jones EY. Structural basis for plexin activation and regulation. *Neuron*. 2016; 91:548–560. [PubMed: 27397516]
- Korn MJ, Mandle QJ, Parent JM. Conditional disabled-1 deletion in mice alters hippocampal neurogenesis and reduces seizure threshold. *Front. Neurosci*. 2016; 10:63. [PubMed: 26941603]
- Li G, Pleasure SJ. Morphogenesis of the dentate gyrus: what we are learning from mouse mutants. *Dev. Neurosci*. 2005; 27:93–99. [PubMed: 16046842]
- Li G, Kataoka H, Coughlin SR, Pleasure SJ. Identification of a transient subpial neurogenic zone in the developing dentate gyrus and its regulation by Cxcl12 and reelin signaling. *Development*. 2009; 136:327–335. [PubMed: 19103804]
- Li G, Fang L, Fernández G, Pleasure SJ. The ventral hippocampus is the embryonic origin for adult neural stem cells in the dentate gyrus. *Neuron*. 2013; 78:658–672. [PubMed: 23643936]
- Lilja J, Zacharchenko T, Georgiadou M, Jacquemet G, De Franceschi N, Peuhu E, Hamidi H, Pouwels J, Martens V, Nia FH, et al. SHANK proteins limit integrin activation by directly interacting with Rap1 and R-Ras. *Nat. Cell Biol*. 2017; 19:292–305. [PubMed: 28263956]
- Liu M, Pleasure SJ, Collins AE, Noebels JL, Naya FJ, Tsai MJ, Lowenstein DH. Loss of BETA2/NeuroD leads to malformation of the dentate gyrus and epilepsy. *Proc. Natl. Acad. Sci. USA*. 2000; 97:865–870. [PubMed: 10639171]
- Mah S, Nelson MR, Delisi LE, Reneland RH, Markward N, James MR, Nyholt DR, Hayward N, Handoko H, Mowry B, et al. Identification of the semaphorin receptor PLXNA2 as a candidate for susceptibility to schizophrenia. *Mol. Psychiatry*. 2006; 11:471–478. [PubMed: 16402134]
- Maren S. Neurobiology of Pavlovian fear conditioning. *Annu. Rev. Neurosci*. 2001; 24:897–931. [PubMed: 11520922]
- Mosca-Boidron AL, Gueneau L, Huguet G, Goldenberg A, Henry C, Gigot N, Palesi-Pocachard E, Falace A, Duplomb L, Thevenon J, et al. A de novo microdeletion of SEMA5A in a boy with autism spectrum disorder and intellectual disability. *Eur. J. Hum. Genet*. 2016; 24:838–843. [PubMed: 26395558]

- Nicola Z, Fabel K, Kempermann G. Development of the adult neurogenic niche in the hippocampus of mice. *Front. Neuroanat.* 2015; 9:53. [PubMed: 25999820]
- Oinuma I, Ishikawa Y, Katoh H, Negishi M. The Semaphorin 4D receptor Plexin-B1 is a GTPase activating protein for R-Ras. *Science.* 2004; 305:862–865. [PubMed: 15297673]
- Pasterkamp RJ. Getting neural circuits into shape with semaphorins. *Nat. Rev. Neurosci.* 2012; 13:605–618. [PubMed: 22895477]
- Perez-Branguli F, Zagar Y, Shanley DK, Graef IA, Chédotal A, Mitchell KJ. Reverse signaling by Semaphorin-6A regulates cellular aggregation and neuronal morphology. *PLoS ONE.* 2016; 11:e0158686. [PubMed: 27392094]
- Powell SB, Weber M, Geyer MA. Genetic models of sensorimotor gating: relevance to neuropsychiatric disorders. *Curr. Top. Behav. Neurosci.* 2012; 12:251–318. [PubMed: 22367921]
- Puüschel AW. GTPases in semaphorin signaling. *Adv. Exp. Med. Biol.* 2007; 600:12–23. [PubMed: 17607943]
- Renaud J, Kerjan G, Sumita I, Zagar Y, Georget V, Kim D, Fouquet C, Suda K, Sanbo M, Suto F, et al. Plexin-A2 and its ligand, Sema6A, control nucleus-centrosome coupling in migrating granule cells. *Nat. Neurosci.* 2008; 11:440–449. [PubMed: 18327254]
- Renoux AJ, Sala-Hamrick KJ, Carducci NM, Frazer M, Halsey KE, Sutton MA, Dolan DF, Murphy GG, Todd PK. Impaired sensorimotor gating in Fmr1 knock out and Fragile X premutation model mice. *Behav. Brain Res.* 2014; 267:42–45. [PubMed: 24657592]
- Riccomagno MM, Kolodkin AL. Sculpting neural circuits by axon and dendrite pruning. *Annu. Rev. Cell Dev. Biol.* 2015; 31:779–805. [PubMed: 26436703]
- Rickmann M, Amaral DG, Cowan WM. Organization of radial glial cells during the development of the rat dentate gyrus. *J. Comp. Neurol.* 1987; 264:449–479. [PubMed: 3680638]
- Rohm B, Rahim B, Kleiber B, Hovatta I, Puüschel AW. The semaphorin 3A receptor may directly regulate the activity of small GTPases. *FEBS Lett.* 2000; 486:68–72. [PubMed: 11108845]
- Rouillet FI, Crawley JN. Mouse models of autism: testing hypotheses about molecular mechanisms. *Curr. Top. Behav. Neurosci.* 2011; 7:187–212. [PubMed: 21225409]
- Ruücker AE, O'Tuathaigh C, Dunleavy M, Morris DW, Little GE, Corvin AP, Gill M, Henshall DC, Waddington JL, Mitchell KJ. Mutation of Semaphorin-6A disrupts limbic and cortical connectivity and models neurodevelopmental psychopathology. *PLoS ONE.* 2011; 6:e26488. [PubMed: 22132072]
- Sahay A, Kim CH, Sepkuty JP, Cho E, Hagan RL, Ginty DD, Kolodkin AL. Secreted semaphorins modulate synaptic transmission in the adult hippocampus. *J. Neurosci.* 2005; 25:3613–3620. [PubMed: 15814792]
- Saito Y, Oinuma I, Fujimoto S, Negishi M. Plexin-B1 is a GTPase activating protein for M-Ras, remodelling dendrite morphology. *EMBO Rep.* 2009; 10:614–621. [PubMed: 19444311]
- Schizophrenia Working Group of the Psychiatric Genomics Consortium. Biological insights from 108 schizophrenia-associated genetic loci. *Nature.* 2014; 511:421–427. [PubMed: 25056061]
- Shah B, Lutter D, Tsytsyura Y, Glyvuk N, Sakakibara A, Klingauf J, Puüschel AW. Rap1 GTPases are master regulators of neural cell polarity in the developing neocortex. *Cereb. Cortex.* 2017; 27:1253–1269. [PubMed: 26733533]
- Shimonaka M, Katagiri K, Nakayama T, Fujita N, Tsuruo T, Yoshie O, Kinashi T. Rap1 translates chemokine signals to integrin activation, cell polarization, and motility across vascular endothelium under flow. *J. Cell Biol.* 2003; 161:417–427. [PubMed: 12707305]
- Stornetta RL, Zhu JJ. Ras and Rap signaling in synaptic plasticity and mental disorders. *Neuroscientist.* 2011; 17:54–78. [PubMed: 20431046]
- Sun LO, Jiang Z, Rivlin-Etzion M, Hand R, Brady CM, Matsuoka RL, Yau KW, Feller MB, Kolodkin AL. On and off retinal circuit assembly by divergent molecular mechanisms. *Science.* 2013; 342:1241974. [PubMed: 24179230]
- Sun LO, Brady CM, Cahill H, Al-Khindi T, Sakuta H, Dhande OS, Noda M, Huberman AD, Nathans J, Kolodkin AL. Functional assembly of accessory optic system circuitry critical for compensatory eye movements. *Neuron.* 2015; 86:971–984. [PubMed: 25959730]

- Suto F, Tsuboi M, Kamiya H, Mizuno H, Kiyama Y, Komai S, Shimizu M, Sanbo M, Yagi T, Hiromi Y, et al. Interactions between plexinA2, plexin-A4, and semaphorin 6A control lamina-restricted projection of hippocampal mossy fibers. *Neuron*. 2007; 53:535–547. [PubMed: 17296555]
- Swerdlow NR, Weber M, Qu Y, Light GA, Braff DL. Realistic expectations of prepulse inhibition in translational models for schizophrenia research. *Psychopharmacology (Berl.)*. 2008; 199:331–388. [PubMed: 18568339]
- Takeshita M, Yamada K, Hattori E, Iwayama Y, Toyota T, Iwata Y, Tsuchiya KJ, Sugihara G, Hashimoto K, Watanabe H, et al. Genetic examination of the PLXNA2 gene in Japanese and Chinese people with schizophrenia. *Schizophr. Res.* 2008; 99:359–364. [PubMed: 18065206]
- Tamminga CA, Stan AD, Wagner AD. The hippocampal formation in schizophrenia. *Am. J. Psychiatry*. 2010; 167:1178–1193. [PubMed: 20810471]
- Tawarayama H, Yoshida Y, Suto F, Mitchell KJ, Fujisawa H. Roles of semaphorin-6B and plexin-A2 in lamina-restricted projection of hippocampal mossy fibers. *J. Neurosci.* 2010; 30:7049–7060. [PubMed: 20484647]
- Toritsuka M, Kimoto S, Muraki K, Landek-Salgado MA, Yoshida A, Yamamoto N, Horiuchi Y, Hiyama H, Tajinda K, Keni N, et al. Deficits in microRNA-mediated Cxcr4/Cxcl12 signaling in neurodevelopmental deficits in a 22q11 deletion syndrome mouse model. *Proc. Natl. Acad. Sci. USA*. 2013; 110:17552–17557. [PubMed: 24101523]
- Tran TS, Rubio ME, Clem RL, Johnson D, Case L, Tessier-Lavigne M, Hagan RL, Ginty DD, Kolodkin AL. Secreted semaphorins control spine distribution and morphogenesis in the postnatal CNS. *Nature*. 2009; 462:1065–1069. [PubMed: 20010807]
- Wang Y, He H, Srivastava N, Vikarunnessa S, Chen YB, Jiang J, Cowan CW, Zhang X. Plexins are GTPase-activating proteins for Rap and are activated by induced dimerization. *Sci. Signal*. 2012; 5:ra6. [PubMed: 22253263]
- Wang Y, Pascoe HG, Brautigam CA, He H, Zhang X. Structural basis for activation and non-canonical catalysis of the Rap GTPase activating protein domain of plexin. *eLife*. 2013; 2:e01279. [PubMed: 24137545]
- Weiss KH, Johanssen C, Tielsch A, Herz J, Deller T, Frotscher M, Förster E. Malformation of the radial glial scaffold in the dentate gyrus of reeler mice, scrambler mice, and ApoER2/VLDLR-deficient mice. *J. Comp. Neurol.* 2003; 460:56–65. [PubMed: 12687696]
- Weiss LA, Arking DE, Daly MJ, Chakravarti A. Gene Discovery Project of Johns Hopkins & the Autism Consortium. A genome-wide linkage and association scan reveals novel loci for autism. *Nature*. 2009; 461:802–808. [PubMed: 19812673]
- Williams ME, Wilke SA, Daggett A, Davis E, Otto S, Ravi D, Ripley B, Bushong EA, Ellisman MH, Klein G, Ghosh A. Cadherin-9 regulates synapse-specific differentiation in the developing hippocampus. *Neuron*. 2011; 71:640–655. [PubMed: 21867881]
- Wray NR, Gottesman II. Using summary data from the danish national registers to estimate heritabilities for schizophrenia, bipolar disorder, and major depressive disorder. *Front. Genet.* 2012; 3:118. [PubMed: 22783273]
- Wray NR, James MR, Mah SP, Nelson M, Andrews G, Sullivan PF, Montgomery GW, Birley AJ, Braun A, Martin NG. Anxiety and comorbid measures associated with PLXNA2. *Arch. Gen. Psychiatry*. 2007; 64:318–326. [PubMed: 17339520]
- Yang M, Silverman JL, Crawley JN. Automated three-chambered social approach task for mice. *Curr. Protoc. Neurosci.* 2011; (Unit 8.26) Chapter 8.
- Yin DM, Chen YJ, Sathyamurthy A, Xiong WC, Mei L. Synaptic dysfunction in schizophrenia. *Adv. Exp. Med. Biol.* 2012; 970:493–516. [PubMed: 22351070]
- Yoo SK, Pascoe HG, Pereira T, Kondo S, Jacinto A, Zhang X, Hariharan IK. Plexins function in epithelial repair in both *Drosophila* and zebrafish. *Nat. Commun.* 2016; 7:12282. [PubMed: 27452696]

Highlights

- Sema5A-PlexinA2 signaling regulates dentate granule cell progenitor migration
- PlexinA2 GAP activity and Rap1 small GTPases direct progenitor migration
- *Plxna2* function is required for the formation of the DG neurogenic niche
- *Plxna2-GAP* deficiency disrupts contextual fear memory and sensorimotor gating

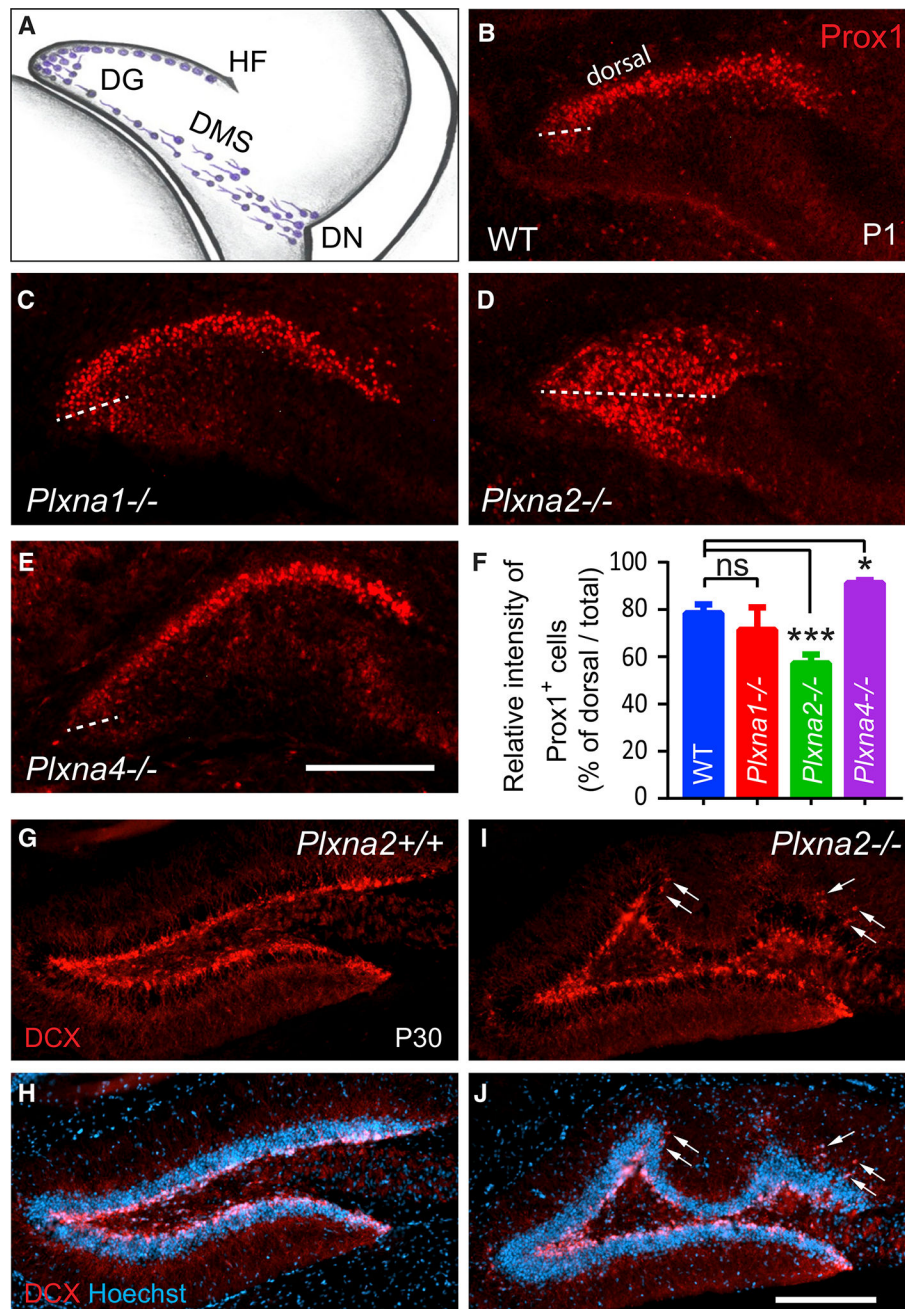


Figure 1. *Plxna2* and *Plxna4* Regulate GC Distribution in the Developing DG

(A) In the developing mouse DG, immature GCs (blue cells) migrate from the dentate notch (DN) of the telencephalic neuroepithelium, along the dentate migratory stream (DMS) toward the hippocampal fissure (HF).

(B–E) Anti-Prox1 staining of coronal brain sections through the rostral pole of the P1 hippocampus of (B) WT (n = 4), (C) *Plxna1*^{-/-} (n = 3), (D) *Plxna2*^{-/-} (n = 5), and (E) *Plxna4*^{-/-} (n = 3) pups. The border between the dorsal and ventral GCL is marked by a dotted line through the medial pole of the DG.

(F) Quantification of Prox1⁺ cells in the dorsal blade of the GCL compared to total Prox1 (GCL + hilus) labeling. Results are shown as mean value \pm SD. * $p < 0.05$; *** $p < 0.001$, by one-way ANOVA, with Dunn *post hoc* t test. ns, not significant.

(G–J) Coronal sections through the dorsal hippocampus of P30 (G and H) *Plxna2*^{+/+} (n = 3) and littermate (I and J) *Plxna2*^{-/-} mice (n = 3) stained with anti-DCX (G and I) and with anti-DCX + Hoechst dye 33342 (H and J). Arrows point to ectopically positioned DCX⁺ cells in the dentate molecular layer. Scale bar, 200 μ m.

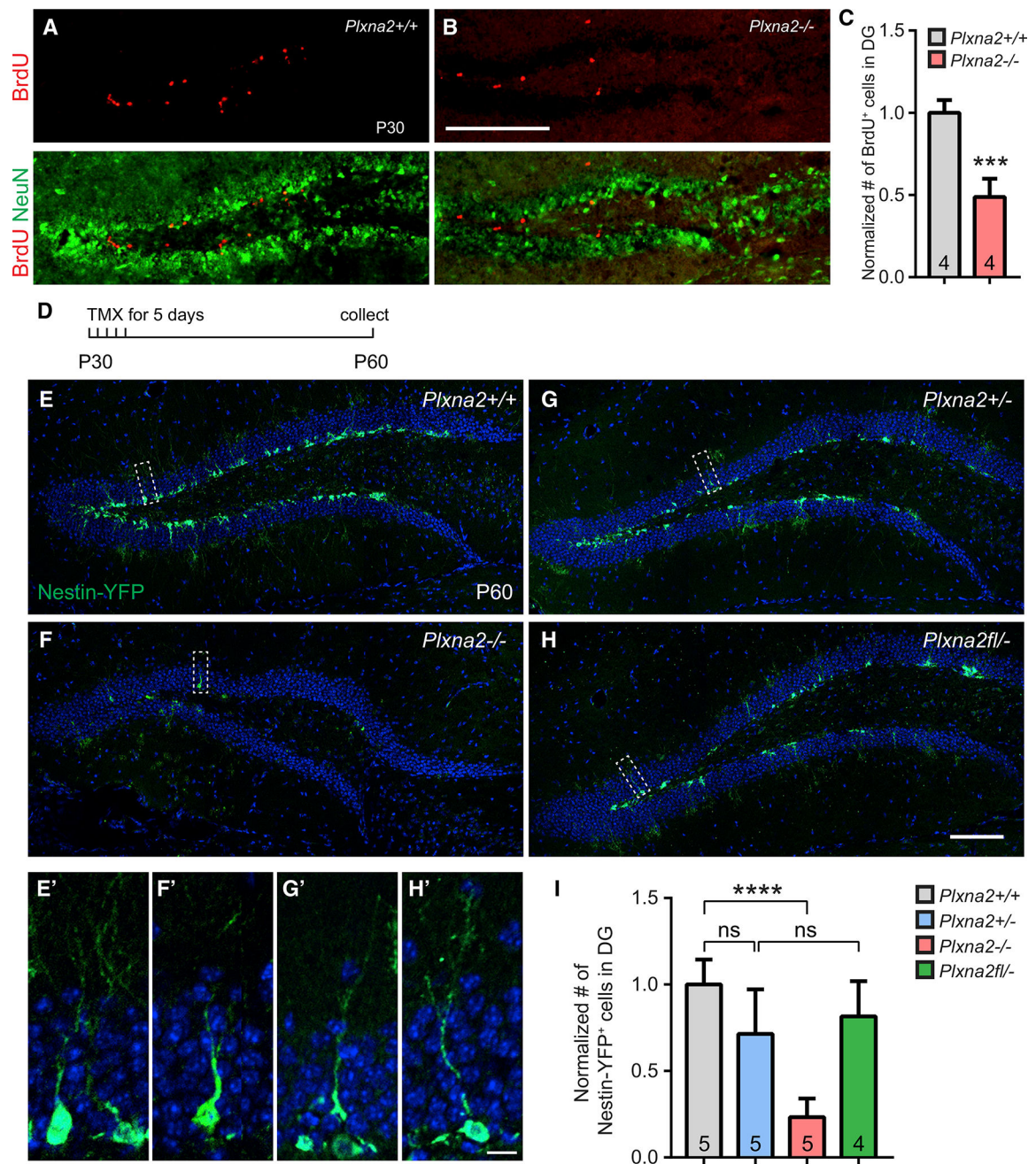


Figure 2. *Plxna2* Regulates Cell Proliferation and Formation of the Stem Cell Niche in the SGZ (A and B) Coronal brain sections through the dorsal DG of P30 (A) *Plxna2*^{+/+} (n = 4) and (B) *Plxna2*^{-/-} (n = 4) mice, stained with anti-BrdU and anti-NeuN.

(C) Quantification of BrdU⁺ cells. Results are shown as mean value ± SD. ***p < 0.001, by unpaired two-tailed Student's t test.

(D–I) Fate mapping of nestin⁺ cells in the DG of *Nestin-Cre-ERT2/R26R:YFP* mice.

(D) Timeline of tamoxifen (TMX) administration and tissue collection.

(E–H) Coronal brain sections through the dorsal DG of P60 (E) *Plxna2*^{+/+} (n = 5), (F) *Plxna2*^{-/-} (n = 5), (G) *Plxna2*^{+/-} (n = 5), and (H) *Plxna2*^{fl/-} conditional knockout (n = 4)

mice on a *Nestin-Cre-ER^{T2}/R26R:YFP* background. Progeny of nestin⁺ cells were visualized by anti-GFP immunofluorescence, and sections were counterstained with the Hoechst dye 33342.

(E'–H') Higher magnifications of boxed areas shown in (E)–(H).

(I) Quantification of GFP⁺ cells normalized to cell counts (100%) in *Plxna2^{+/+}* mice. Results are shown as mean value \pm SD. **** $p < 0.0001$, one-way ANOVA, with Bonferroni *post hoc* t test. ns, not significant.

Scale bars, 200 μ m in (B), 100 μ m in (H), and 10 μ m in (H').

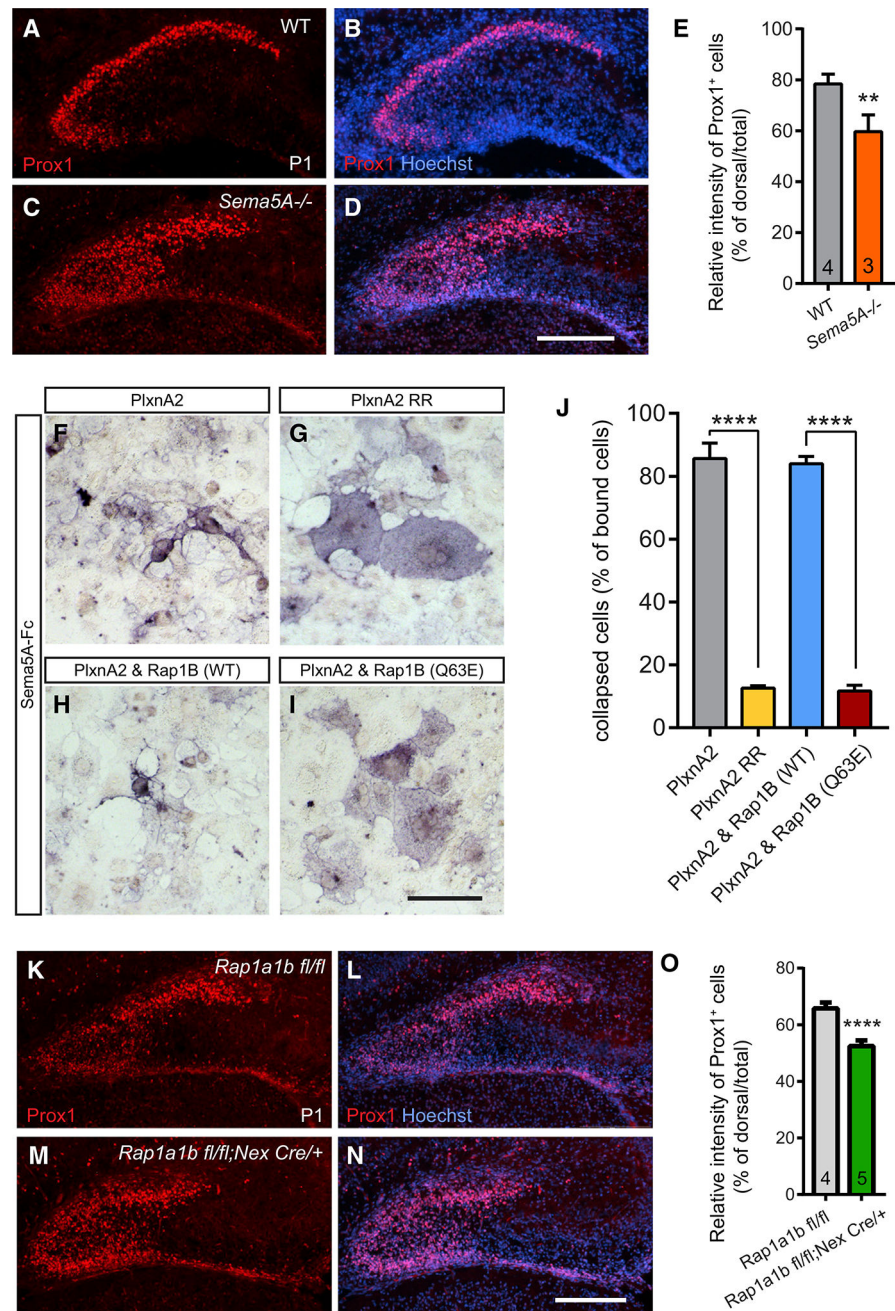


Figure 3. Sema5A and the Small GTPase Rap1 Are Required for Proper GC Migration
 (A–D) Anti-Prox1 staining of coronal brain sections through the dorsal hippocampus of P1 (A and B) WT (n = 4) and (C and D) *Sema5A*^{-/-} (n = 3) mouse pups.
 (E) Quantification of GC distribution defects. Results are shown as mean value ± SD. **p < 0.01, unpaired two-tailed Student's t test.
 (F–I) Binding of Sema5A-Fc fusion protein to COS7 cells expressing recombinant (F) WT PlxnA2, (G) PlxnA2 RR, (H) WT PlxnA2 and WT Rap1B, and (I) PlxnA2 and constitutively active Rap1B(Q63E).
 (K–N) Anti-Prox1 staining of coronal brain sections through the dorsal hippocampus of P1 (K and L) *Rap1a1b* fl/fl and (M and N) *Rap1a1b* fl/fl; *Nex Cre*^{+/+} mouse pups.
 (O) Quantification of GC distribution defects. Results are shown as mean value ± SD. ****p < 0.0001, unpaired two-tailed Student's t test.

(J) Quantification of the percentile of collapsed cells of total number of Sema5A-Fc binding cells (n = 3 independent experiments).

(K–N) Anti-Prox1 staining of coronal brain sections through the dorsal hippocampus of P1 (K and L) *Rap1a^{flox/flox}/Rap1b^{flox/flox}* (n = 4) and (M and N) *Rap1a^{flox/flox}/Rap1b^{flox/flox};Nex-Cre* (n = 5) mouse pups.

(O) Quantification of GC distribution. Results are shown as mean value \pm SD. ****p < 0.0001, unpaired two-tailed Student's t test.

Scale bars, 200 μ m in (D) and (N) and 100 μ m in (I).

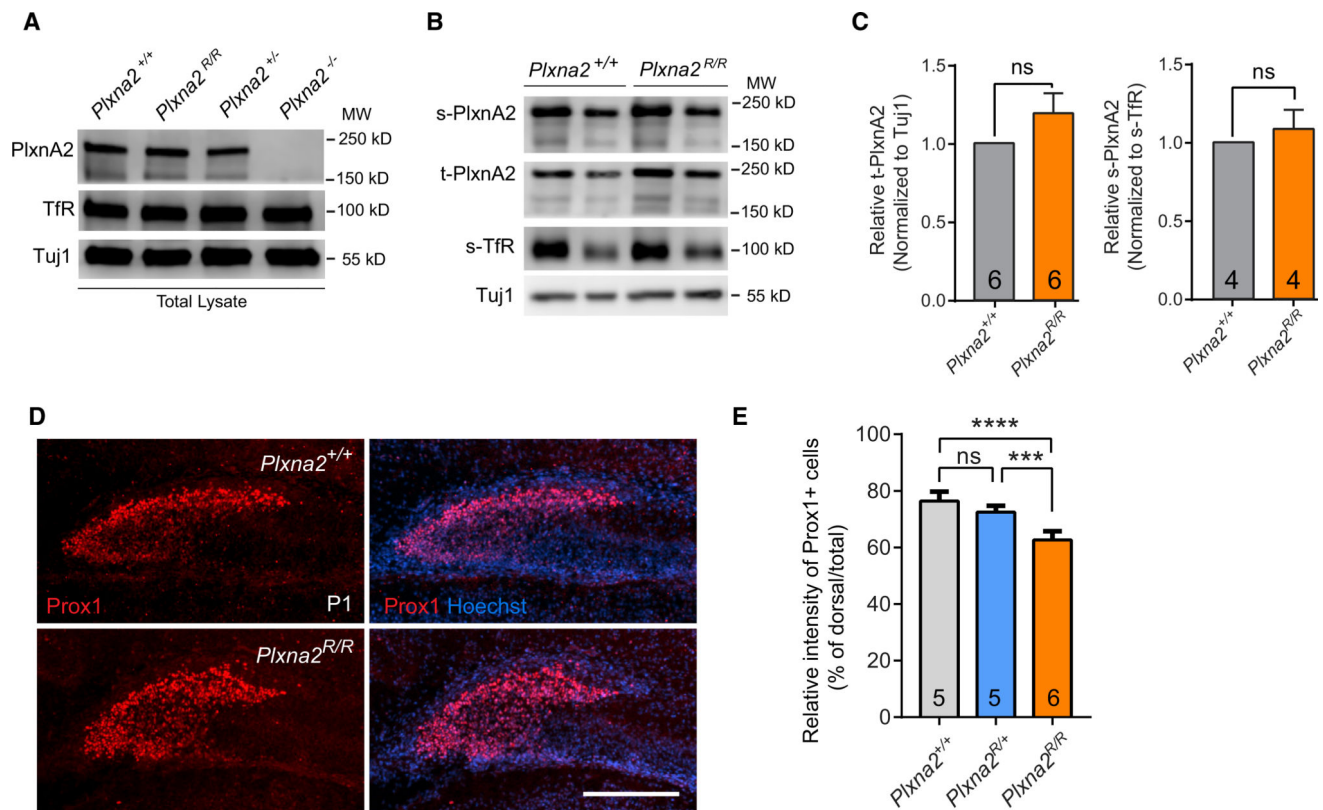


Figure 4. PlxnA2 GAP Forward Signaling Is Required for Proper Distribution of GCs in the Developing DG

(A and B) Western blot analysis of mouse forebrain cell-culture lysates. (A) Blots of total cell lysates of *PlxnA2*^{+/+}, *PlxnA2*^{R/R}, *PlxnA2*^{+/-}, and *PlxnA2*^{-/-} DIV10 (10 days in vitro) cultures and (B) biotinylated cell-surface proteins isolated from *PlxnA2*^{+/+} and *PlxnA2*^{R/R} cultures probed with anti-PlxnA2, anti-TfR, TuJ1, t-PlxnA2 (total PlxnA2), or s-PlxnA2 (surface PlxnA2).

(C) Quantification of t-PlxnA2 in *PlxnA2*^{+/+} and *PlxnA2*^{R/R} lysates normalized to TuJ1 (left; n = 6) and s-PlxnA2 normalized to s-TfR (right; n = 4). Data are shown as mean ± SEM, unpaired two-tailed Student's t test.

(D) Anti-Prox1 staining of coronal brain sections through the dorsal hippocampus of P1 (A) *PlxnA2*^{+/+} (n = 5) and *PlxnA2*^{R/R} (n = 6) mouse pups. Scale bar is 200 μm.

(E) Quantification of GC distribution in the *PlxnA2*^{+/+} (n = 5), *PlxnA2*^{R/+} (n = 5), and *PlxnA2*^{R/R} (n = 6) DG. Results are shown as mean value ± SD. ***p < 0.001; ****p < 0.0001, one-way ANOVA with Tukey *post hoc* t test. ns, not significant.

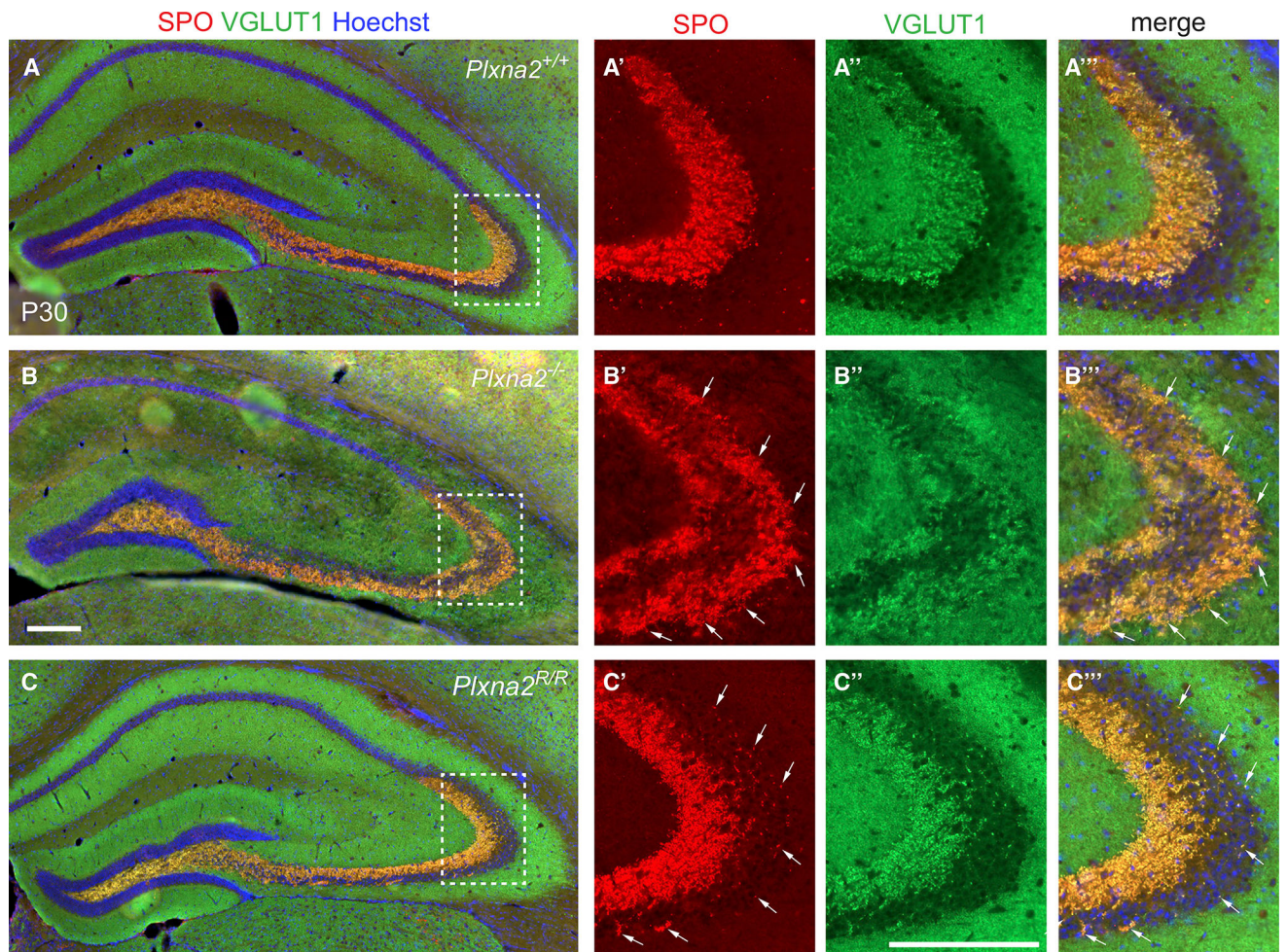


Figure 5. PlxnA2 GAP Activity Is Not Required for Mossy Fiber-CA3 Targeting and Mossy Fiber Bouton Formation

(A–C'') Representative examples of coronal brain sections through the dorsal DG of P30 (A) *Plxna2*^{+/+} (n = 4), (B) *Plxna2*^{-/-} (n = 4), and (C) *Plxna2*^{R/R} (n = 4) mice, stained for the presynaptic markers SPO and anti-VGLUT1 to visualize MFBs. (A'–C'') High magnification of the dotted regions shown in (A)–(C). Arrows in (B')–(B'') and (C')–(C'') point to ectopic MFBs in the stratum pyramidale in *Plxna2*^{-/-} and *Plxna2*^{R/R} mice. Scale bars, 200 μ m.

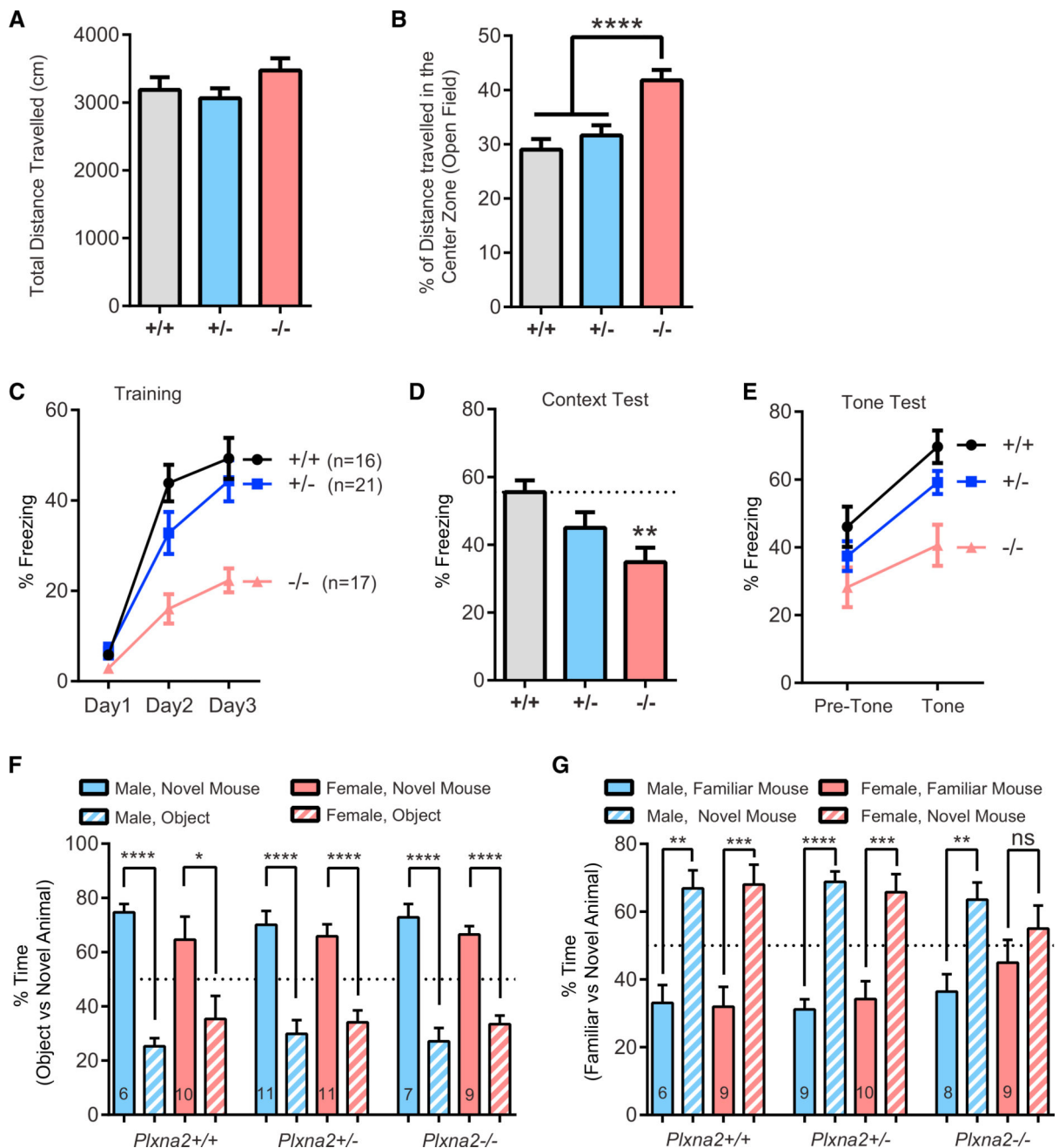


Figure 6. Loss of *Plxna2* Impairs Contextual Fear Memory and Sociability

(A) Quantification of total distance traveled in the OFT for *Plxna2*^{+/+} (n = 16), *Plxna2*^{+/-} (n = 22), and *Plxna2*^{-/-} (n = 16) mice; F(2, 52) = 1.591, p = 0.9739.

(B) Percentage of total distance traveled in the center zone of the OFT chamber; F(2, 52) = 11.28, p < 0.0001. Data represent mean ± SEM. ****p < 0.0001, one-way ANOVA with Tukey's correction for multiple comparisons.

(C) Prior to training, *Plxna2*^{+/+} (n = 16), *Plxna2*^{+/-} (n = 19), and *Plxna2*^{-/-} (n = 16) mice all exhibited similar levels of freezing on day 1 (one-way ANOVA: F(2, 48) = 2.448, p = 0.100). All groups exhibited increased freezing levels across 3 days of cued fear

conditioning, $F(2, 96) = 102.362$, $p < 0.0001$; however, a repeated-measures ANOVA reveals that *Plxna2*^{-/-} mice exhibit reduced freezing levels compared to their *Plxna2*^{+/+} and *Plxna2*^{+/-} littermates (effect of genotype: $F(2, 48) = 15.996$, $p < 0.0001$; Genotype × Training interaction: $F(4, 96) = 5.715$, $p = 0.0004$).

(D) When returned to the original training context after 24 hr, *Plxna2*^{-/-} mice exhibit reduced freezing levels during a 5-min context exposure, compared to their *Plxna2*^{+/+} littermates ($F(2, 51) = 5.399$, $p = 0.0075$, one-way ANOVA with Tukey's correction for multiple comparisons).

(E) Freezing in response to tone was assessed 48 hr after training. When analyzed using a two-factor repeated-measures ANOVA, all groups exhibited an increase in freezing in response to a tone (effect of training: $F(1, 47) = 76.352$, $p < 0.0001$). While there was a main effect of genotype ($F(2, 47) = 5.715$, $p = 0.0053$), the Genotype × Training interaction did not reach statistical significance ($F(1, 47) = 2.415$, $p = 0.1004$).

(F and G) Three-chambered social interaction test: (F) both male and female *Plxna2*^{+/+}, *Plxna2*^{+/-}, and *Plxna2*^{-/-} mice spent significantly more time engaged in nose-to-nose interaction with an unfamiliar mouse than with an inanimate object (unpaired t test). (G) All mice spent significantly more time engaged in nose-to-nose interaction with a novel mouse than with a familiar mouse, except for female *Plxna2*^{-/-} mice, which showed no preference (unpaired t test). Number of mice tested is shown in bar graphs.

Data represent mean ± SEM. * $p < 0.05$; ** $p < 0.01$; *** $p < 0.001$; **** $p < 0.0001$. ns, not significant.

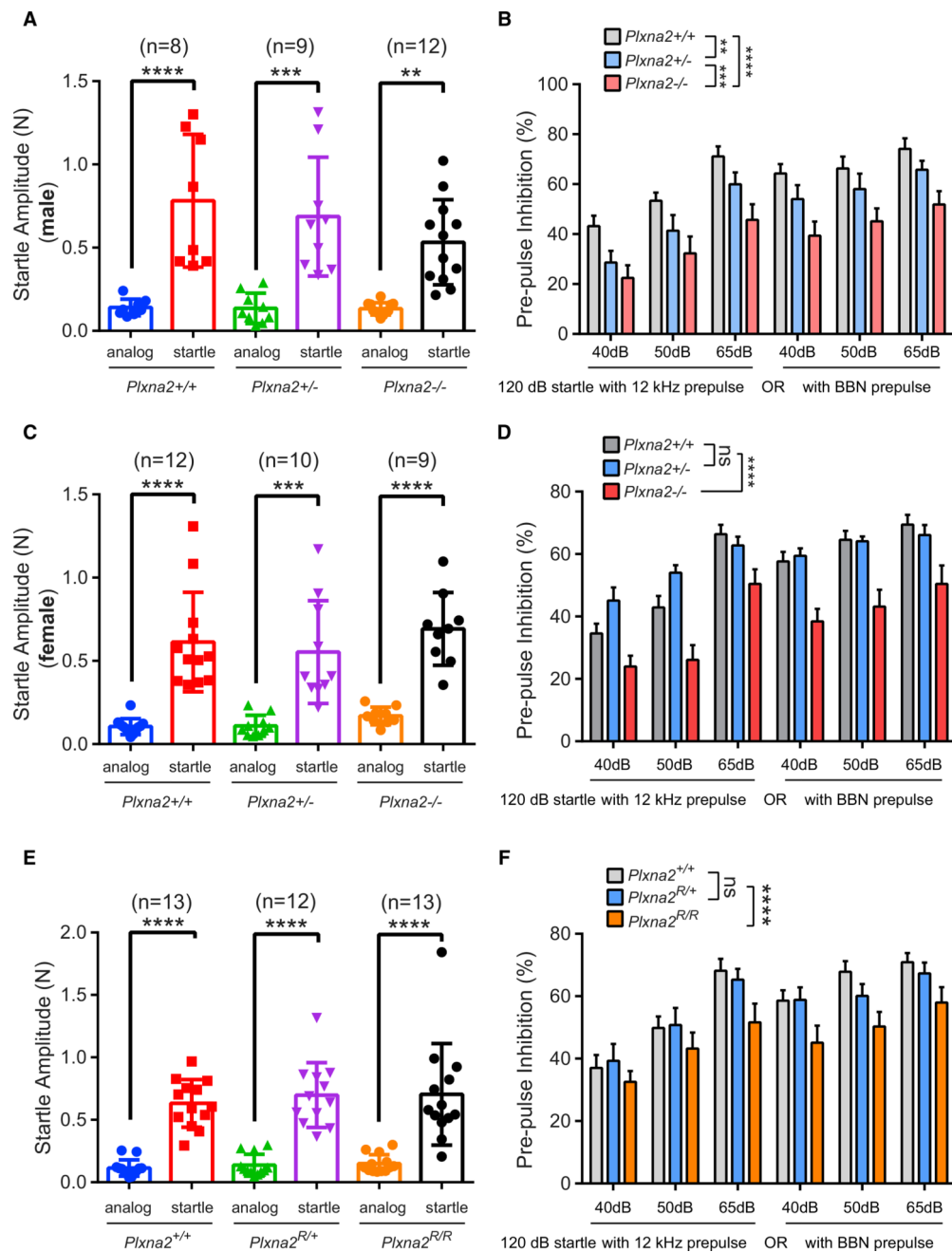


Figure 7. Defective Sensorimotor Gating in *Plxna2*^{-/-} and *Plxna2*^{R/R} Mice

(A) Testing of the startle amplitude of male *Plxna2*^{+/+} (n = 8), *Plxna2*^{+/-} (n = 9), and *Plxna2*^{-/-} (n = 12) mice to a 120-dB sound.

(B) Percentile of PPI of the same cohort of mice with a prepulse delivered at 12 kHz or as broadband noise (BBN) at 40, 50, and 65 dB prior to the 120-dB startle sound.

(C) Testing of the startle amplitude of female *Plxna2*^{+/+} (n = 12), *Plxna2*^{+/-} (n = 10), and *Plxna2*^{-/-} (n = 9) mice to a 120-dB sound.

(D) Percentile of PPI of the same cohort of mice with a prepulse delivered at 12 kHz or as BBN at 40, 50, and 65 dB prior to the 120-dB startle sound.

(E) Testing of the startle amplitude of *Plxna2^{+/+}* (n = 13), *Plxna2^{R/+}* (n = 12), and *Plxna2^{R/R}* (n = 13) mice to a 120-dB sound.

(F) Percentile of PPI of the same cohort of mice with a prepulse delivered at 12 kHz or as BBN at 40, 50, and 65 dB prior to the 120-dB startle sound.

Data are presented as mean \pm SD in (A), (C), and (E); **p < 0.01, ***p < 0.001, and ****p < 0.0001, by one-way ANOVA, with Tukey *post hoc* t test. Error bars indicate SEM in (B), (D), and (F); **p < 0.01, ***p < 0.001, and ****p < 0.0001, by two-way ANOVA, with Fisher's least significant difference (LSD). ns, not significant.